Contrib Mineral Petrol (1996) 123: 263–281

Charles R. Stern · Rolf Kilian

Role of the subducted slab, mantle wedge and continental crust in the generation of adakites from the Andean Austral Volcanic Zone

Received: 1 March 1995 / Accepted: 13 September 1995

Abstract All six Holocene volcanic centers of the Andean Austral Volcanic Zone (AVZ; 49–54°S) have erupted exclusively adakitic andesites and dacites characterized by low Yb and Y concentrations and high Sr/Y ratios, suggesting a source with residual garnet, amphibole and pyroxene, but little or no olivine and plagioclase. Melting of mafic lower crust may be the source for adakites in some arcs, but such a source is inconsistent with the high Mg# of AVZ adakites. Also, the AVZ occurs in a region of relatively thin crust (<35 km) within which plagioclase rather than garnet is stable. The source for AVZ adakites is more likely to be subducted oceanic basalt, recrystallized to garnet-amphibolite or eclogite. Geothermal models indicate that partial melting of the subducted oceanic crust is probable below the Austral Andes due to the slow subduction rate (2 cm/year) and the young age (<24 Ma) of the subducted oceanic lithosphere. Geochemical models for AVZ adakites are also consistent with a large material contribution from subducted oceanic crust (35–90% slab-derived mass), including sediment (up to 4% sediment-derived mass, representing approximately 15% of all sediment subducted). Variable isotopic and trace-element ratios observed for AVZ adakites, which span the range reported for adakites world-wide, require multistage models involving melting of different proportions of subducted basalt and sediment, as well as an important material contribution from both the overlying mantle wedge (10–50% mass contribution) and continental crust (0–30% mass contribution). Andesites from Cook Island volcano, located in the southernmost AVZ (54°S) where subduction is more oblique, have MORB-like Sr, Nd, Pb and O isotopic composition and trace-element ratios. These can be modeled by small degrees (2–4%) of partial melting of eclogitic MORB, yielding a tonalitic parent (intermediate SiO_2, $CaO/Na_2O>1$), followed by limited interaction of this melt with the overlying mantle (≥90% MORB melt, ≤10% mantle), but only very little (≤1%) or no participation of either subducted sediment or crust. In contrast, models for the magmatic evolution of Burney (52°S), Reclus (51°S) and northernmost AVZ (49–50°S) andesites and dacites require melting of a mixture of MORB and subducted sediment, followed by interaction of this melt not only with the overlying mantle, but the crust as well. Crustal assimilation and fractional crystallization (AFC) processes and the mass contribution from the crust become more significant northwards in the AVZ as the angle of convergence becomes more orthogonal.

C.R. Stern (✉)
Department of Geological Science, University of Colorado, Boulder, CO 80309-0250, USA

R. Kilian
Mineralogisches Institut, Universität Heidelberg, Im Neuenheimer Feld 236, D-69120 Heidelberg, Germany

Editorial responsibility: T.L. Grove

Introduction

Possible sources for convergent plate boundary magmas include subducted oceanic crust, the overlying mantle wedge and the arc crust. Green and Ringwood (1968) suggested direct partial melting of subducted ocean-floor basalts transformed to eclogites to produce the calc-alkaline andesites that occur within many arcs. Later experimental (Stern 1974) and geochemical (Gill 1981) studies concluded that most calc-alkaline andesites are unlikely to be direct partial melts of subducted mid-ocean ridge basalt (MORB). However, some recent studies of subduction zone magmatism have again invoked an important role for slab-melting in the generation of certain calc-alkaline andesites and dacites, termed adakites (Defant and Drummond 1990). Compared to normal calc-alkaline andesites and dacites, adakites have distinctive chemical characteristics suggesting derivation by partial melting of basalt transformed to garnet-amphibolite and/or eclogite.

Adakitic andesites and dacites have been identified in a number of arc segments globally, including both the type locality on Adak Island as well as further west in the

Aleutians (Kay 1978; Yogodzinski et al. 1995), in the southernmost Andes (Stern et al. 1984; Futa and Stern 1988; Kay et al. 1993), in both the Baja, Mexico (Rogers et al. 1985) and Panamanian (Defant et al. 1991a,b) portions of the Central American arc, in Japan (Morris 1995) and in the Cascade volcanic range of the northwestern United States (Defant and Drummond 1993). Although not volumetrically significant on a global scale, the implications of the distinctive chemistry of adakites has motivated renewed attention to the role of melting of subducted oceanic crust in the evolution of arc magmas, both presently (Peacock et al. 1994; Sen and Dunn 1994) and during the Archean (Drummond and Defant 1990; Rapp et al. 1991; Martin 1993).

One of the arc segments in which adakitic andesites and dacites were first identified and attributed to melting of subducted oceanic basalts was the Andean Austral Volcanic Zone (AVZ, Fig. 1; Stern et al. 1984). All six volcanoes in the AVZ have erupted andesites and dacites with adakitic chemical characteristics as identified by Defant and Drummond (1990), but these volcanoes also exhibit significant chemical differences among themselves, which span the range of different types of adakites identified world-wide. This paper discusses the chemical differences among AVZ volcanoes and their genesis within the context of the regional tectonics and geology of the southern Andes.

Regional geology and tectonics

The volcanoes of the AVZ result from the subduction of young (12–24 Ma) Antarctic plate below southernmost South America at low convergence velocities of 2 cm/year (Fig. 1; Cande and Leslie 1986). The AVZ is separated from the Andean Southern Volcanic Zone (SVZ) by a gap in active volcanism just south of the Chile Rise-Trench triple junction, below which even younger (<6 Ma) oceanic crust is being subducted. West of the active volcanoes of the AVZ, the age of the subducted plate entering the trench changes from 12 Ma in the north to 24 Ma in the south. The convergence direction, which is nearly orthogonal at the latitude of the northernmost volcano in the AVZ (Lautaro, 49°S), becomes increasingly oblique and finally changes to strike-slip plate motion south of the southernmost volcano in the AVZ (Cook Island, 54°S). Compared to the other volcanoes in the AVZ, the Cook Island volcanic center is located further from the trench along the direction of plate convergence.

The southern margin of South America is cut by a system of transform faults, the most important being the Malvinas Chasm Fault which merges westwards with the Magallanes Fault Zone (Fig. 1; Fuenzalida 1974; Herron et al. 1977). Forsyth (1975) defined a small microplate, the Scotia plate, south of this fault system. The southern tip of South America and the Cook Island volcano lie on this microplate.

Seismicity is negligible south of the Chile Rise-Trench triple junction, possibly because of both the slow rate of convergence and the young age of the oceanic plate (Forsyth 1975), which may cause the subducted slab to be several hundreds of degrees hotter than in more typical subduction environments (Peacock et al. 1994). Because of the lack of seismicity, the geometry of the sub-

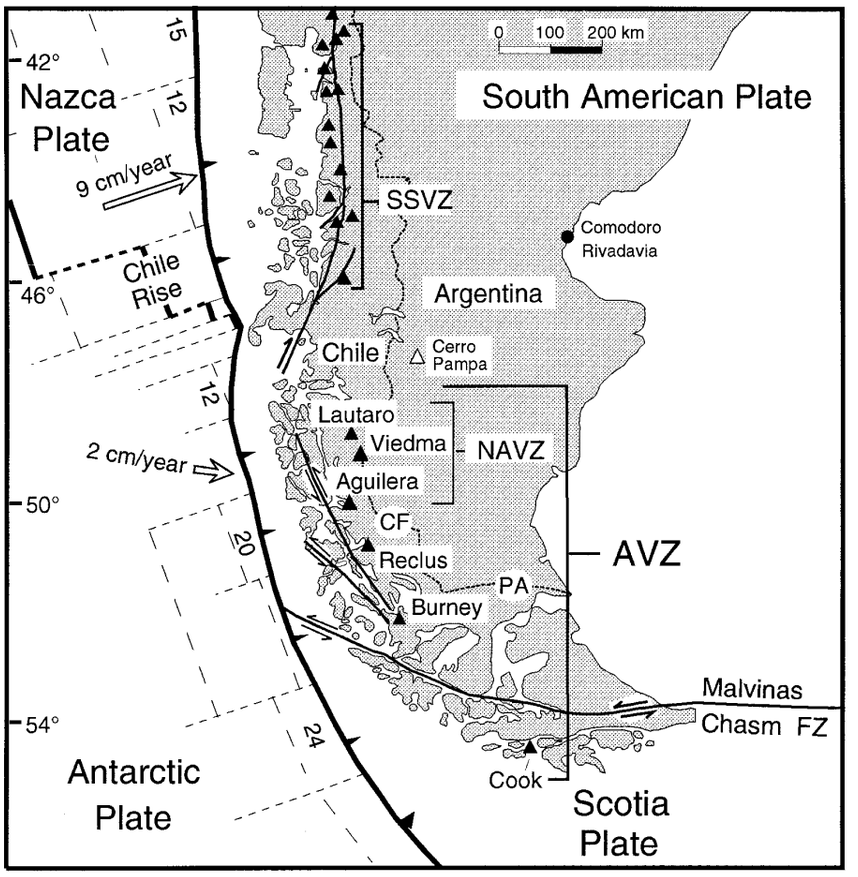

Fig. 1 Location map of the volcanic centers of the Andean Austral Volcanic Zone (*AVZ*). Also shown are the southern Southern Volcanic Zone (*SSVZ*) north of the Chile Rise-Trench triple junction, the late Miocene volcano Cerro Pampa (*CP*) in Argentina that erupted adakitic magmas (Kay et al. 1993), and lower-crustal and mantle xenolith localities within the Patagonian plateau basalts (*CF* Cerro del Fraile, Kilian 1995; *PA* Pali-Aike, Selverstone and Stern 1983, Stern et al. 1989). Plate boundaries, plate convergence rates and ages of the oceanic lithosphere (in Ma) are from Forsyth (1975) and Cande and Leslie (1986)

ducted slab and mantle wedge below the AVZ cannot be determined.

The southernmost Andes consist of Late Paleozoic to Early Mesozoic metamorphic basement, Mesozoic and Cenozoic mafic (Rocas Verdes ophiolites), intermediate (Patagonian batholith) and silicic (Tobifera volcanics) igneous rocks, as well as sedimentary rocks deformed and uplifted beginning in the Middle to Late Cretaceous (Bruhn and Dalziel 1977). In the region of the AVZ, no systematic north-to-south change is known to occur in either the age of the metamorphic basement or the proportion of basement and younger igneous rocks. The southernmost volcano of the AVZ, located on Cook Island, directly overlies plutons of the Patagonian batholith, and Burney, Reclus and Aguilera volcanoes occur along the eastern margin of the batholith. The two northernmost volcanoes in the AVZ, Lautaro and Viedma, occur within the area of the Patagonian ice cap and the details of their bedrock geology is unknown.

Base elevations of AVZ volcanoes are less than a few hundred meters above sea level, and summit elevations of these volcanoes and other peaks of the southernmost Andes are generally less than 3,000 m. This suggests crustal thickness of <35 km, similar to below the southern Andes everywhere south of 36°S (Ramos and Kay 1992; Kay et al. 1993). Xenoliths of lower crustal origin, found in the Patagonian plateau basalts both along (CF, Fig. 1; Kilian 1995) and east of (PA, Fig. 1; Selverstone and Stern 1983) the eastern margin of the Austral Andes, are pyroxene + plagioclase granulites without garnet, consistent with a relatively thin crust.

The Chile Rise was subducted below the Austral Andes during the late Miocene, resulting in the development of a "slab-window" and extensive basaltic plateau volcanism in southern Patagonia prior to the reinitiation of subduction and AVZ arc magmatism (Ramos and Kay 1992). Ridge subduction may have also caused subduction erosion along the continental margin. As noted by Cande and Leslie (1986), the western edge of the Patagonian batholith lies much closer to the trench south compared to north of the Chile Rise-Trench triple junction. Bruhn and Dalziel (1977) also commented on the very narrow arc-trench gap west of the southernmost Patagonian batholith, as well as the fact that the batholith, including plutons as young as mid-Miocene, has been deeply exposed, yet no post-Paleozoic accretionary belt of any type has been formed. These authors have suggested that both subduction of significant amounts of terrigenous sediment and/or subduction erosion of the continental margin must be invoked to explain the enormous amount of missing continental crust in this region. Some of this subduction erosion may have occurred since the formation of the mid-Miocene plutonic belt, because plutons in this belt south of the Chile Rise-Trench triple junction are located closer to the axis of the present trench than those north of the triple junction. Cande and Leslie (1986) suggest that active subduction erosion is occurring in conjuction with the subduction of the Chile Rise at 46°S, and presumably also occurred west of the AVZ as the locus of subduction of this spreading ridge migrated northwards during the Miocene.

Cook Island volcano consists of a group of nested post-glacial domes (Puig et al. 1984; Heusser et al. 1990). All the other AVZ volcanic centers are glaciated composite stratovolcanoes, for which tephra records imply Holocene activity (Stern 1990; Kilian et al. 1991). Lautaro is the only center with a well documented historic eruption, which occurred in 1959 (Martinic 1988). Only Cook Island and Burney have been mapped in detail, largely because of the logistic problems involved. However, with the exception of Viedma and Lautaro, which are the least accessible, the samples analyzed for this paper were selected from collections made on multiple field excursions conducted independently by the co-authors. For this reason, two of the most significant observations concerning the AVZ, the lack of rocks more mafic than andesites and the near uniformity of petrochemistry observed within individual centers compared to inter-volcano petrochemical variations, are believed to be inherent aspects of these centers, not artifacts of the extent of field sampling.

Analytical techniques

Mineral chemistry was determined with a Cameca Camebax SX-50 electron microprobe (Heidelberg University) using a 15 kV accelerating voltage, a 10 nA beam current, a beam width of 1 μm and a counting time of 20 s (15 s for Na and K).

Whole-rock major element compositions were determined by standard wet-chemical techniques at Skyline Labs (Denver, Colorado). Trace-elements Rb, Sr, Y, Zr and Nb were determined using a Kevex 0700 EDS system (University of Colorado). Based on repeated analysis of standard BHVO-1, precision is estimated at better than 5% for Rb, Sr, Y and Zr and better than 10% for Nb. Samples were also analyzed by INAA at both the Oregon State University Radiation center and Karlsruhe University. Precision is better than 2% for Sc, Ta, La, Sm and Eu, 2–5% for Cr, Ni, Zn, Hf, Th, Ce, Nd, Tb, Yb and Lu, and 10% for Cs, Ba and U.

Sr- and Nd-isotopic compositions, and Rb, Sr, Nd and Sm concentrations, were determined by mass-spectrometry at the United States Geological Survey (Denver, Colorado). Techniques are described in Peng et al. (1986). Precision is 1% for Rb, Sr, Nd and Sm contents. $^{87}Sr/^{86}Sr$ ratios were normalized to $^{86}Sr/^{88}Sr = 0.1194$. $^{87}Sr/^{86}Sr$ determined for the Eimer and Amand $SrCO_3$ standard was 0.70803 ± 0.00005. Precision for $^{87}Sr/^{86}Sr$ is 0.01%. $^{143}Nd/^{144}Nd$ ratios were normalized to $^{144}Nd/^{146}Nd = 0.7219$. $^{143}Nd/^{144}Nd$ for U.S.G.S. standard BCR-1 was 0.512643 ± 0.000011. Precision for $^{143}Nd/^{144}Nd$ is 0.005%. No age correction was applied to the measured Sr- and Nd-isotopic ratios.

Pb-isotopic compositions were determined at Dartmouth College by B. Barreiro (Barreiro 1983). O-isotopic compositions were determined at the University of Alberta by K. Muehlenbachs (Muehlenbachs and Clayton 1972).

Petrography

The essential mineralogy of all the AVZ volcanoes involves pyroxenes, amphibole and plagioclase (Fig. 2). Both a greater proportion of crustal xenoliths and larger more complexly zoned phenocrysts are observed from south-to-north, suggesting increasing importance of near surface magma chamber processes such as slow cooling and crystallization, magma mixing, wall-rock assimilation, and volatile degassing. The petrographic and mineral chemistry variations for each individual center, from south-to-north, are detailed in the following sub-sections.

Cook Island

Andesites of Cook Island have subhedral and euhedral phenocrysts (typically from 0.2–2.5 mm, some as large as 5 mm) of amphibole (6–12 vol.%) and clinopyroxene (3–8 vol.%). Clinopyroxene phenocrysts have broad cores with high Mg# [$Mg/(Mg + Fe^{2+}) \times 100 = 88–94$; Fig. 2], Cr_2O_3 (0.9 to 1.9 wt%) and Cr/(Cr+Al) (Fig. 3), similar to the cores of pyroxenes in Aleutian adakites (Yogodzinski et al. 1995). These high Mg# clinopyroxenes have narrow rims exhibiting strong normal zonation (Mg# = 88–72; Fig. 2), or are enclosed in amphibole. Comparision with clinopyroxenes in garnet- and spinel-peridotite, olivine-websterite and lower-crustal pyroxene-plagioclase-granulite xenoliths found in Patagonian plateau basalts (Fig. 3) suggests that these high Mg# clinopyroxene cores may be xenocrysts derived from the mantle. However, their Al_2O_3 (1.8 to 3.9 wt%) and Na_2O (0.4 to 0.7 wt%) contents are similar only to clinopyroxenes in infertile harzburgite xenoliths, but lower than those in fertile lherzolite xenoliths (Stern et al. 1989). Amphibole phenocrysts also display normal zonation patterns, but with lower Mg# ranges (Mg# = 86–75). The cores of amphiboles are often corroded and rims are partly oxidized due to loss of water during magma uprise and extrusion. Cook Island andesites do not contain either plagioclase, orthopyroxene or olivine phenocrysts.

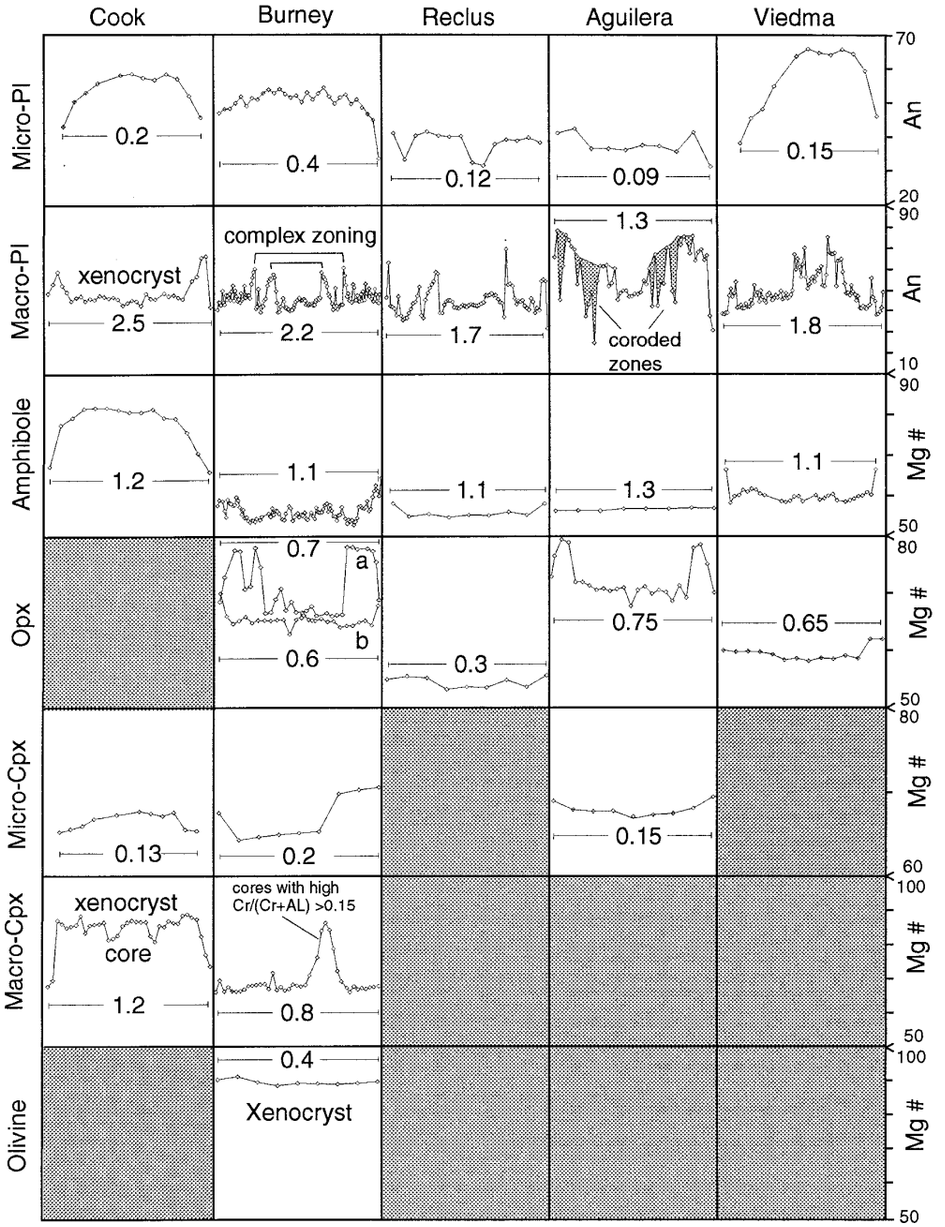

Fig. 2 Summary of chemical zonations (Mg# for mafic minerals; An content for feldspars) of crystals in AVZ adakites. Scale bars indicate profile lengths (in mm)

Plagioclase and clinopyroxene microlites occur in the groundmass of Cook Island andesites. Both are characterized by normal zonation. Plagioclase microlites evolve from An_{68} to An_{35} and clinopyroxene from Mg# = 75 to 68 (Fig. 2). Very small grains of groundmass plagioclase reach An_{25}. The groundmass also contains Fe-Ti oxides, but no orthopyroxene or olivine. Dacitic groundmass glass has enhanced Na_2O contents (up to 6.5 wt%). Cook Island andesites have rare felsic xenoliths and corroded xenocrysts (<1 vol.%) consisting mainly of plagioclase (An_{45}).

Burney

Phenocrysts of Burney andesites and dacites include plagioclase (0.3–2.5 mm), orthopyroxene (0.5–1.3 mm) and clinopyroxene (0.3–1.1 mm). Plagioclase phenocrysts (15–20 vol.%) are euhedral with irregular zoning in the range $An_{45–70}$ (Fig. 2). High anorthite zones are partly corroded. Euhedral orthopyroxenes (Mg# = 61–73; 2–5 vol.%) are less abundant, while partially corroded clinopyroxene (Mg# = 73–78; 1–2 vol.%) phenocrysts have both normal and reversly zoned rims. Some clinopyroxenes have cores with high Mg# (Mg#>90; Fig. 2) and Cr/(Cr + Al) (Fig. 3), similar to the cores of Cook Island clinopyroxenes. Corroded olivine grains (Fo_{91}; Fig. 2), with NiO = 0.3 to 0.5 wt%, were also observed associated with high Mg# clinopyroxenes in small aggregates. Amphibole also occurs in Burney andesites and dacites, but only rarely.

The groundmass of Burney rocks contain variable amounts of plagioclase ($An_{60–35}$) and orthopyroxene (Mg#≤60) microlites, opaques, and glass of dacitic to rhyolitic composition. Small (<4 mm) xenoliths of upper crustal granitoids and greenschists are present (<2 vol.%).

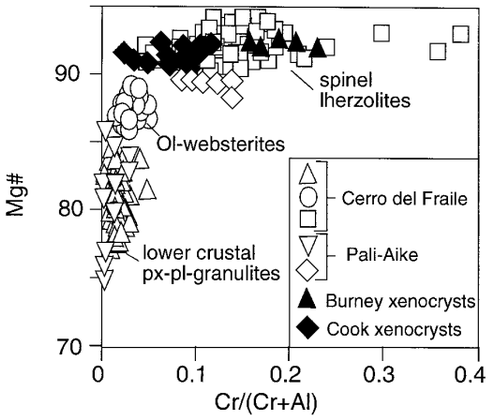

Fig. 3 Mg# versus Cr/(Cr+Al) for cores of clinopyroxenes from Cook Island and Burney andesites compared to clinopyroxenes from mantle-derived garnet- and spinel-peridotite and olivine-websterite xenoliths and lower-crustal pyroxene-plagioclase-granulite xenoliths found in the Cerro del Fraile (*CF*, Fig. 1; Kilian 1995) and Pali-Aike (*PA*, Fig. 1; Selverstone and Stern 1983, Stern et al. 1989) basalts east of the Austral Andes

Reclus

Phenocrysts of Reclus dacites consist mainly of euhedral plagioclase (0.3 to 6 mm; 17–25 vol.%), with variable core compositions (An_{42-62}), and often irregular zoning with abrupt changes from An_{35} to An_{65} (Fig. 2). High anorthite zones (>An_{60}) are typically corroded. Less abundant amphibole phenocrysts (2–3 vol.%) are strongly corroded, and partly oxidized or recrystallized to orthopyroxene, suggesting extensive water loss in the uppermost crust. Euhedral and subhedral orthopyroxene (0.2–0.6 mm; <1 vol.%; Mg# = 65–55) may be formed during late-stage crystallization.

The groundmass consists of variable proportions of plagioclase grains and microlites of orthopyroxene, sometimes hornblende, and glass. Groundmass glass has dacitic to rhyolitic composition, with variable K content produced by either local heterogeneities during crystallization or magma mixing. Xenoliths and xenocrysts are more common in Reclus dacites than in those of Burney. They consist mainly of corroded quartz and plagioclase grains (up to 3 mm; 2–4 vol.%).

Northern AVZ volcanoes

Dacites of the three northernmost AVZ volcanoes (NAVZ; Fig. 1) display certain petrographic characteristics in common. Subhedral plagioclase (0.2–4 mm) is the most abundant phenocryst (8–12 vol.%). Zoning is very complex, including normal, reverse, and irregular zones suggesting a complex intra-crustal crystallization history. For example, some plagioclase of Aguilera show a systematic inverse zoning from An_{40} to An_{75} (Fig. 2), whereas some at Viedma have a normal zonation from An_{75} to An_{40}. Subhedral amphibole phenocrysts (0.3–3 mm) are characteristic of all NAVZ dacites, but less abundant (1–3 vol.%) than plagioclase. Amphibole is usually corroded and/or rimmed by orthopyroxene. Biotite also occurs in these volcanoes (<1%). Small euhedral orthopyroxene phenocrysts (Mg# = 65) are common. In addition, in the dacites of Aguilera, clinopyroxene occurs as microphenocryst (0.2–0.6 mm) characterized by both high-Mg cores (Mg# = 72) and reversly zoned rims (Mg# = 81).

The groundmass of all the NAVZ volcanoes includes variable proportions of plagiocalse (An_{50-28}; Or_{1-7}), orthopyroxene, Fe-Ti oxides, and rhyolitic glass with K_2O contents ranging from 3.2 to 4.5 wt%. Granitic and granodioritic xenoliths are common (2–4 vol.%).

Geochemistry

All samples from the AVZ are andesites and dacites (Table 1; Figs. 4, 5), which in common with typical orogenic andesites and dacites have high Al and low Ti. However, they have relatively high Mg# compared to more typical arc andesites and dacites, including those from the Andean SVZ north of the Chile Rise-Trench triple junction (Fig. 4; Stern et al. 1984; Futa and Stern 1988). Another significant feature of the AVZ centers is the lack of basalts or basaltic andesites, which are the dominant rock type erupted from the volcanic centers in the Andean SVZ.

All the AVZ andesites and dacites have chemical characteristics which would identify them as adakites. As outlined by Defant and Drummond (1990, 1993) these characteristics include: SiO_2>56 wt%, Al_2O_3>15 wt%, low HREE (Yb<1.9 ppm) and Y<18 ppm, high Sr>400 ppm and Sr/Y>40, and positive Sr and Eu anomalies. These characteristics have been interpreted to reflect both the presence of residual garnet and absence of plagioclase in the source region of adakites (Defant and Drummond 1990; Peacock et al. 1994).

AVZ andesites and dacites also have low concentrations of high field strength elements (HFSE), which is a

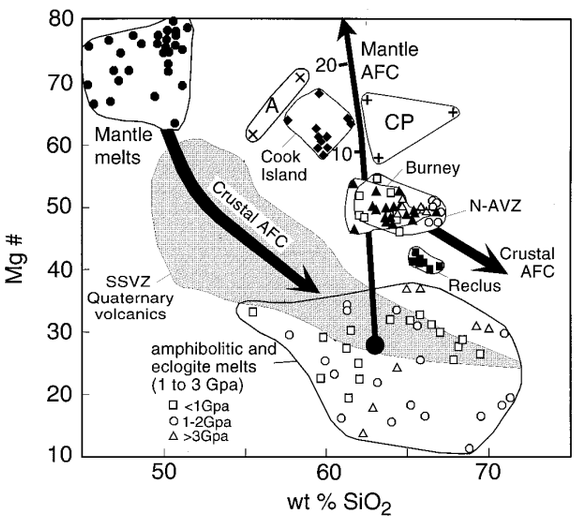

Fig. 4 Mg# versus wt% SiO_2 for AVZ andesites and dacites compared to experimentally produced high pressure partial melts of garnet-amphibolite and eclogite (Table 2; Keleman 1995), mantle melts (basalts), Quaternary volcanic rocks from the Andean southern Southern Volcanic Zone (*SSVZ*, Fig. 1; Lopez-Escobar et al. 1993), and adakites from Adak Island, Aleutians (*A*; Kay 1978) and Cerro Pampa, Argentina (*CP*; Kay et al. 1993). Curve for mantle AFC was calculated following DePaolo (1981) with a mass-assimilation/fractionation ratio of r = 2, reflecting a relatively hot mantle wedge, and 80% amphibole + 20% clinopyroxene as fractionating phases

Table 1 Major and trace element, and isotopic compositions of samples from the volcanoes in the Andean Austral volcanic zone

Sample	Lautaro						Viedma		Aguilera			
	La-1	La-2	La-3	La-4	Lau-5	La-N1	Vd-1	Vd-3	Ag-1	Ag-2	Ag-5	Ag-7
SiO_2	66.78	67.02	66.91	66.56	66.30	66.60	64.63	65.94	63.99	64.36	62.35	62.04
TiO_2	0.59	0.51	0.59	0.52	0.59	0.54	0.63	0.60	0.68	0.60	0.79	0.79
Al_2O_3	16.61	17.24	16.11	17.04	16.09	16.71	16.91	16.76	17.16	16.54	16.61	16.59
FeO	3.53	3.50	3.87	3.45	3.82	3.60	4.21	3.94	4.51	4.01	5.43	5.46
MnO	0.07	0.09	0.07	0.09	0.07	0.10	0.08	0.07	0.09	0.09	0.09	0.09
MgO	2.05	1.91	1.97	2.02	1.95	2.02	2.37	2.18	2.79	2.09	2.87	2.91
CaO	4.32	3.77	4.12	3.80	4.47	4.47	4.97	4.88	5.58	4.93	5.71	5.72
Na_2O	3.76	3.22	3.41	3.06	3.73	3.70	3.68	3.68	4.22	4.20	4.17	4.11
K_2O	2.20	1.98	2.18	2.15	2.12	2.09	1.84	1.89	2.12	2.04	2.09	2.16
P_2O_5	0.11	0.23	0.13	0.19	0.17	0.19	0.07	0.12	0.00	0.24	0.23	0.25
H_2O	0.00	0.00	0.26	0.00	0.00	0.00	0.32	0.09	0.00	0.00	0.23	0.23
Sum	100.02	99.47	99.62	98.88	99.31	100.02	99.71	100.15	101.14	99.10	100.57	100.35
Cr	25	24	28	26	25	30	26	27	13	38	28	26
Ni	–	–	11	–	21	0	14	7	–	–	19	18
Sc	10	10	10	10	9	11	10	11	8	13	13	13
V	–	–	79	–	70	–	64	63	–	–	108	103
Zn	–	–	69	–	65	–	67	62	–	–	59	57
K	18263	16437	18097	17848	17607	17350	15274	15689	17599	16935	17350	17931
Rb	59	68	64	61	63	55	52	53	60	57	57	63
Cs	2.04	1.78	1.87	1.71	2.18	1.93	1.85	1.92	1.88	1.70	1.90	1.77
Ba	555	576	543	549	554	564	504	448	535	449	447	444
Sr	500	492	527	496	494	509	600	608	478	470	511	463
Ta	0.67	0.69	0.70	0.62	1.02	0.69	0.59	0.64	0.71	0.66	0.87	0.74
Nb	10	8	9	8	8	8	6	7		5	10	11
Hf	3.9	4.0	4.1	3.7	3.7	4.0	4.0	4.0	3.6	4.1	4.1	4.6
Zr	134	137	156	132	150	140	200	191	131	141	149	150
Ti	3537	3057	3537	3117	3530	3237	3777	3597	4077	3597	4736	4736
Y	13	12	12	13	11	11	16	17	8	8	15	16
Th	11.7	10.8	10.0	11.2	9.3	12.0	9.8	10.0	13.6	11.6	10.4	10.7
U	1.7	1.5	1.9	1.3	1.7	1.7	1.9	1.6	2.3	1.9	1.9	2.5
La	30.4	29.4	30.6	29.7	28.9	36.6	25.8	28.0	31.3	28.5	29.6	29.3
Ce	60.5	56.5	66.6	57.7	56.9	68.9	48.5	52.3	57.6	58.8	59.7	60.1
Nd	19.5	19.8	26.6	20.0	20.7	25.6	17.1	20.2	24.2	19.5	20.0	21.1
Sm	3.3	3.3	3.9	3.6	3.2	4.4	3.0	4.0	3.9	3.4	4.0	4.0
Eu	1.2	1.0	0.9	1.0	0.8	1.3	1.0	1.2	1.2	1.4	1.1	1.1
Tb	0.57	0.65	0.00	0.56	0.00	0.00	0.00	0.00	0.72	0.77	0.66	0.47
Yb	0.99	0.80	0.96	0.83	0.83	1.04	0.98	1.00	1.10	1.20	1.32	1.54
Lu	0.17	0.16	0.15	0.16	0.15	0.19	0.13	0.14	0.22	0.25	0.22	0.19
$\delta^{18}O$	8.3	8.2	–	7.0	–	8.3	–	–	7.5	7.0	7.4	–
$^{87}Sr/^{86}Sr$	0.70541	–	–	0.70511	–	0.70539	0.70521	–	0.70500	0.70495	–	–
$^{143}Nd/^{144}Nd$	0.51254	–	–	–	–	–	0.51259	–	–	0.51269	–	–
$^{206}Pb/^{204}Pb$	18.61	–	–	–	–	–	18.63	–	–	18.66	–	–
$^{207}Pb/^{204}Pb$	15.59	–	–	–	–	–	15.58	–	–	15.56	–	–
$^{208}Pb/^{204}Pb$	38.52	–	–	–	–	–	38.53	–	–	38.52	–	–

Table 1 (continued)

Sample	Reclus				Mt. Burney						Cook Island		
	Re-1	Re-2	Re-4	Re-5	MB-14	MB-7	MB-9	MB-21P	MB-12	MB-1	Ck-3-198	Ck-1-468	Ck-3-197
SiO_2	65.82	67.00	66.40	65.94	63.07	64.17	64.53	69.49	63.81	64.10	59.56	61.36	61.51
TiO_2	0.43	0.40	0.40	0.43	0.49	0.43	0.42	0.34	0.57	0.46	0.78	0.71	0.87
Al_2O_3	16.83	16.60	16.63	16.81	17.69	17.90	17.33	18.25	18.01	18.14	18.35	18.36	18.00
FeO	4.20	3.88	3.92	4.18	4.50	4.03	3.85	3.45	4.12	4.36	3.65	3.46	3.68
MnO	0.09	0.09	0.09	0.09	0.10	0.09	0.09	0.80	0.00	0.09	0.07	0.07	0.07
MgO	1.65	1.49	1.48	1.65	2.80	2.26	2.18	2.15	2.28	2.20	4.42	3.50	3.58
CaO	4.80	4.43	4.50	4.80	5.81	5.79	5.50	5.39	5.81	5.62	8.54	7.80	7.82
Na_2O	4.17	4.19	4.22	4.18	4.60	4.48	4.21	4.71	4.46	4.33	4.51	4.42	4.30
K_2O	1.38	1.53	1.47	1.37	0.87	0.95	1.08	0.93	0.95	0.79	0.60	0.57	0.60
P_2O_5	0.19	0.17	0.17	0.19	0.20	0.21	0.20	0.21	0.00	0.03	0.29	0.30	0.34
H_2O	0.04	0.11	0.00	0.00	0.00	0.00	0.00	0.00	0.00	0.06	0.00	0.00	0.00
Sum	99.59	99.88	99.27	99.64	100.13	100.31	99.39	100.72	100.01	100.18	100.77	100.55	100.77
Cr	10	9	8	9	13	24	21	12	–	11	76	63	53
Ni	–	–	–	–	30	24	21	20	–	20	65	53	47
Sc	7	7	7	7	10	10	9	8	–	9	9	9	9
V	53	46	52	57	–	–	–	–	–	64	76	63	53
Zn	55	52	50	46	–	–	–	–	–	61	–	–	–
K	11447	12668	12203	11381	7222	7886	8965	7720	7886	6558	4981	4732	4981
Rb	28	30	29	29	10	12	13	11	15	9	3	3	3
Cs	0.40	0.51	0.60	0.43	0.16	0.24	0.32	0.28	0.23	0.25	–	–	–
Ba	398	413	417	418	278	319	324	295	300	260	177	124	101
Sr	545	532	534	519	624	626	594	563	605	615	2003	1910	1770
Ta	0.61	0.64	0.54	0.59	–	0.20	0.21	0.40	–	0.35	0.61	0.66	0.55
Nb	7	6	8	6	3	3	3	3	3	2	12	11	9
Hf	3.7	3.6	3.3	3.8	2.5	2.6	2.4	2.4	–	2.5	3.3	3.7	3.8
Zr	149	154	151	164	74	86	83	83	–	145	122	117	137
Ti	2590	2386	2404	2548	2938	2578	2518	2038	3417	2758	4676	4256	5216
Y	10	9	12	11	6	4	6	6	11	10	6	6	4
Th	3.1	3.9	3.6	3.6	1.4	1.7	1.5	1.0	–	1.3	4.4	4.1	4.7
U	1.4	1.0	1.5	1.9	0.9	0.7	0.3	–	–	0.5	1.3	1.3	1.4
La	21.0	20.9	20.5	20.9	10.4	12.6	14.0	10.5	10.1	10.7	35.3	27.9	30.6
Ce	42.7	45.1	41.9	45.9	24.4	28.1	28.3	22.8	21.9	22.0	75.7	63.5	70.4
Nd	22.1	22.2	20.6	24.4	11.6	12.3	12.6	10.1	10.4	9.4	28.1	15.0	27.7
Sm	3.0	2.9	3.0	3.0	2.4	2.6	2.5	2.1	2.2	2.1	4.2	4.6	5.3
Eu	0.7	0.8	0.9	0.8	1.0	0.9	0.9	0.8	0.8	0.8	1.6	1.6	1.7
Tb	0.40	0.38	0.46	0.36	–	–	–	–	–	–	0.64	0.77	–
Yb	1.15	1.20	0.99	1.24	1.36	1.23	0.99	0.89	1.28	1.10	0.99	0.85	1.01
Lu	0.19	0.11	0.16	0.16	0.16	0.18	0.20	0.18	–	0.15	0.03	0.04	0.04
$\delta^{18}O$	–	–	–	–	6.5	7.2	6.9	6.9	6.3	–	5.7	5.5	5.1
$^{87}Sr/^{86}Sr$	–	–	0.70511	–	0.70418	0.70415	0.70426	0.70406	–	–	0.70280	0.70268	–
$^{143}Nd/^{144}Nd$	–	–	0.51257	–	–	–	0.51275	0.51276	–	–	0.51314	–	–
$^{206}Pb/^{204}Pb$	–	–	18.67	–	–	–	18.69	–	–	–	18.50	–	–
$^{207}Pb/^{204}Pb$	–	–	15.58	–	–	–	15.60	–	–	–	15.53	–	–
$^{208}Pb/^{204}Pb$	–	–	38.50	–	–	–	38.48	–	–	–	38.04	–	–

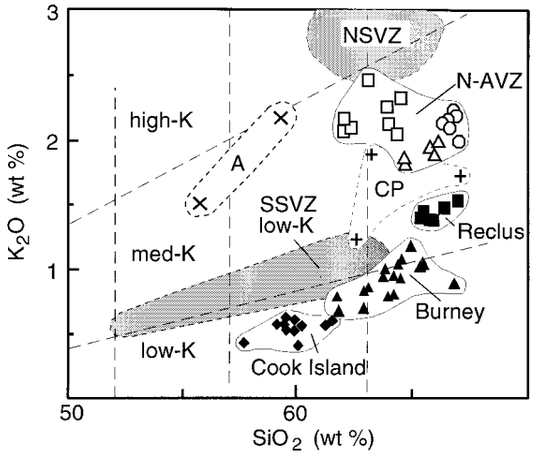

Fig. 5 K_2O versus SiO_2 for samples from the Andean AVZ. Also shown are low-K basalts, basaltic andesites and andesites from the Andean SSVZ (*SSVZ low-K*; Lopez-Escobar et al. 1993), andesites and dacites from the northern SVZ (*NSVZ*; Futa and Stern 1988), and other adakites (*A, CP*; locations and data sources from Fig. 4)

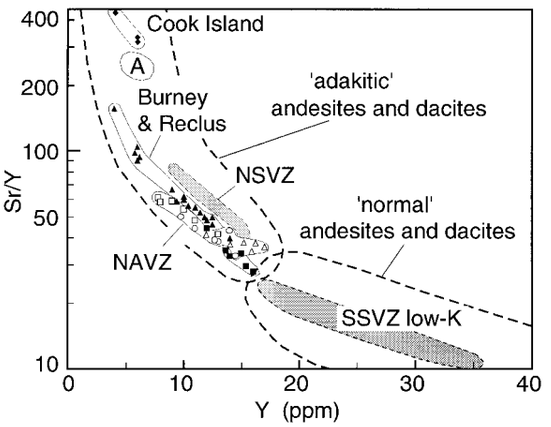

Fig. 6 Sr/Y versus Y for samples from the Andean AVZ. Fields for "adakitic" and "normal" andesites and dacites are from Defant and Drummond (1990). Locations and data sources for other fields (*A, SSVZ low-K, NSVZ*) are from Figs. 4 and 5

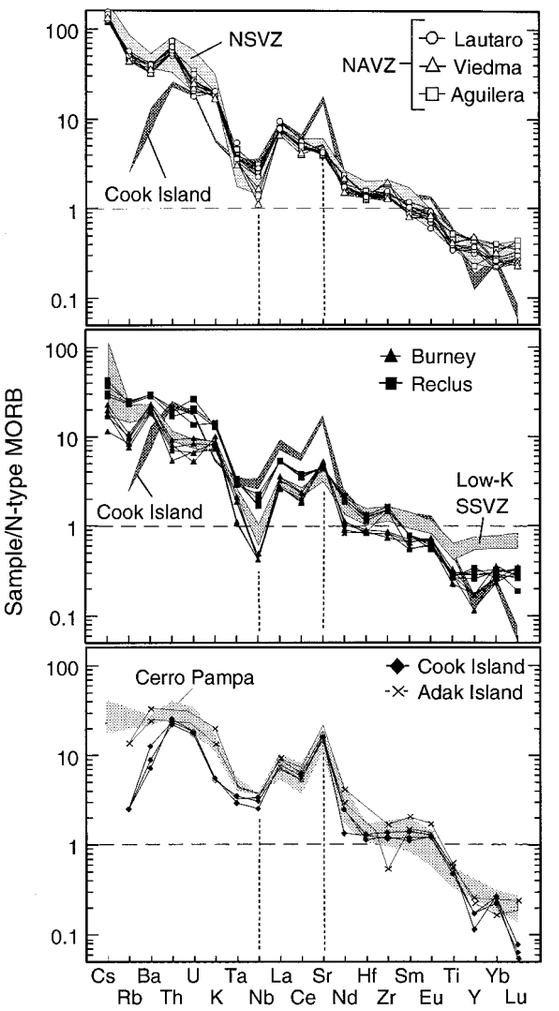

Fig. 7 Spider diagrams of the concentration of trace-elements in samples from the AVZ normalized to N-MORB (Table 3; Sun and McDonough 1989). Locations and data sources for other fields (*Adak Island, Cerro Pampa, low-K SSVZ,* and *NSVZ*) are from Figs. 4 and 5

common feature of both adakites and typical convergent plate boundary magmas. However, other chemical characteristics, such as LREE content, LREE/HREE, large ion lithophile elements (LIL)/LREE, LREE/HFSE and isotopic composition, which may reflect source composition rather than source mineralogy, vary significantly between, but not within, individual centers (Figs. 5–10). As above, we describe the individual centers from south-to-north.

Cook Island

Volcanic rocks of Cook Island are high-CaO (>7.5 wt%), moderate to high-MgO (3.3 to 4.5 wt%; Mg#>60; Fig. 4), low-K_2O (<0.6 wt%; Fig. 5) andesites. Cook Island andesites differ from ordinary orogenic arc andesites by having extraordinarily low Rb (<3 ppm) and Ba (100–180 ppm) and high Sr (>1,750 ppm) concentrations. Specific adakite characteristics of Cook Island andesites include low Y (4–6 ppm; Fig. 6); low HREE (Yb<1.0 ppm; Fig. 7), high Sr (>1,750 ppm), a positive Sr anomaly (Fig. 7) and high Sr/Y (320–440; Fig. 6). Cook Island andesites also have MORB-like Sr, Nd, Pb and O isotopic ratios (Figs. 8–10) and some MORB-like trace-element ratios such as Rb/Sr (<0.002) and Ba/La (<5). However, unlike MORB, they have both high LREE (Fig. 7) and La/Yb (30–36), similar to the type adakite from Adak Island (Kay 1978) and recently described late Miocene adakitic dacites from Cerro Pampa volcano in southern Patagonia (Kay et al. 1993).

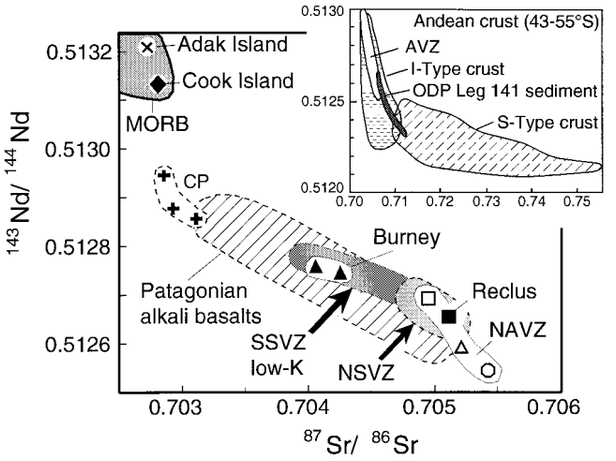

Fig. 8 $^{143}Nd/^{144}Nd$ versus $^{87}Sr/^{86}Sr$ for samples from the Andean AVZ. Field for Patagonian alkali basalts is from Stern et al. (1990) and for MORB is from Sun and McDonough (1989). Location and data sources for other fields (*Adak Island, CP, SSVZ low-K,* and *NSVZ*) are from Figs. 4 and 5. Inset compares AVZ samples to southern South American metamorphic basement (S-Type) and Patagonian batholith (I-Type) crust, as well as Chile Trench sediments sampled in ODP Leg 141 (Behrmann and Kilian 1995)

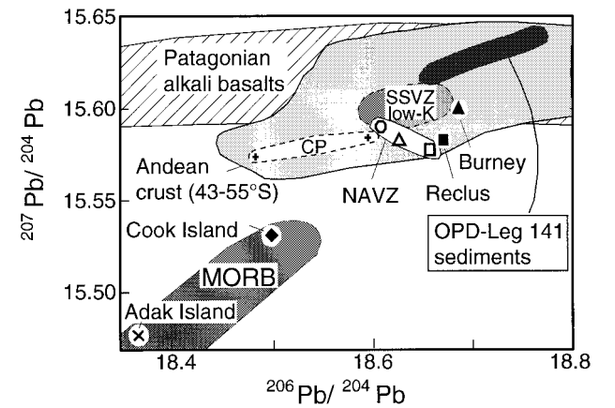

Fig. 9 Pb-isotopic compositions of samples from the volcanoes of the Andean AVZ. Location and data sources for other fields (*MORB, Adak Island, CP, SSVZ low-K, Patagonian alkali basalts, southern South American crust, ODP Leg 141 trench sediments*) are from Figs. 4, 5 and 8

Burney and Reclus

Andesites and dacites from Burney and Reclus (Harambour 1988) volcanoes have lower CaO (<5.8 wt%), MgO (<2.8 wt%; Mg# = 40–53; Fig. 4) and Sr (<630 ppm) and higher K_2O (0.7 to 1.6 wt%; Fig. 5), Ba (230–420 ppm) and Rb (7–30 ppm) than Cook Island andesites. Nevertheless, they have all the characteristics of adakites presented by Defant and Drummond (1990, 1993). HREE and Y are low (Yb<1.36 ppm; Y = 4–13 ppm). Although Sr is not as high as Cook Island andesites, low Y results in high Sr/Y ratios (45–160; Fig. 6). However, even with their low HREE, La/Yb ratios are low (8–21) and not greatly different from normal orogenic andesite, because La contents are low (Fig. 7). Also Ba/La ratios are significantly higher than in Cook Island andesites and more similar to typical arc magmas.

Isotopically, Burney and Reclus andesites and dacites have higher $^{87}Sr/^{86}Sr$ and lower $^{143}Nd/^{144}Nd$ ratios (Fig. 8) than in Cook Island andesites, more similar to other Andean and typical arc andesites. Pb isotopic compositions are also more similar to other Andean andesites and suggests an important crustal or subducted sediment component (Fig. 9). Also $\delta^{18}O$ ratios are higher than in Cook Island andesites (Fig. 10).

Northern AVZ volcanoes

Dacites of the three NAVZ volcanoes have significantly higher K_20 (Fig. 5), Rb, Cs, Th and U concentrations than either Cook Island, Burney or Reclus volcanoes to the south. However, they also have characteristics of adakites such as low HREE (Yb<1.3 ppm) and Y (11–15 ppm; Fig. 7), and high Sr/Y (36–60; Fig. 6). Their La/Yb ratios are also higher than in andesites from Burney and Reclus and more similar to Cook Island andesites (Fig. 7). Ba/La is higher than in Cook Island andesites, but lower than in Burney and Reclus andesites and dacites because of the low La content in the latter. Rb/Sr is significantly higher and K/Rb lower than in Cook Island, Burney or Reclus andesites and dacites.

The Sr- and Nd-isotopic ratios of these volcanoes are higher and lower, respectively, than those to the south (Fig. 8). Pb isotopic compositions are similar to Burney and Reclus (Fig. 9). $\delta^{18}O$ is also higher than in the more southern AVZ volcanoes (Fig. 10). The volcanic centers of the NAVZ have very similar major and trace-element and isotopic chemistry to centers from the northern SVZ (NSVZ, 33–34°S; Figs. 5–10).

Discussion

All the andesites and dacites erupted from AVZ volcanoes share adakitic characteristics such as low HREE and Y and high Sr/Y, but they also exhibit significant geochemical differences in LIL concentration, La/Yb, LIL/LREE and isotopic composition. These differences, particularly the isotopic variations, suggest contributions of variable proportions of different source materials in the generation of different AVZ adakites. As in more typical continental arcs (Kay 1980), subducted oceanic crust (MORB + sediment), the mantle wedge and the continental crust may have contributed to AVZ magmas. We have attempted to model the trace-element and isotopic composition of AVZ magmas on the basis of contributions from these four sources. We discuss the origin of Cook Island andesites first because their chemistry suggests little or no participation of either subducted sediment and/or continental crust.

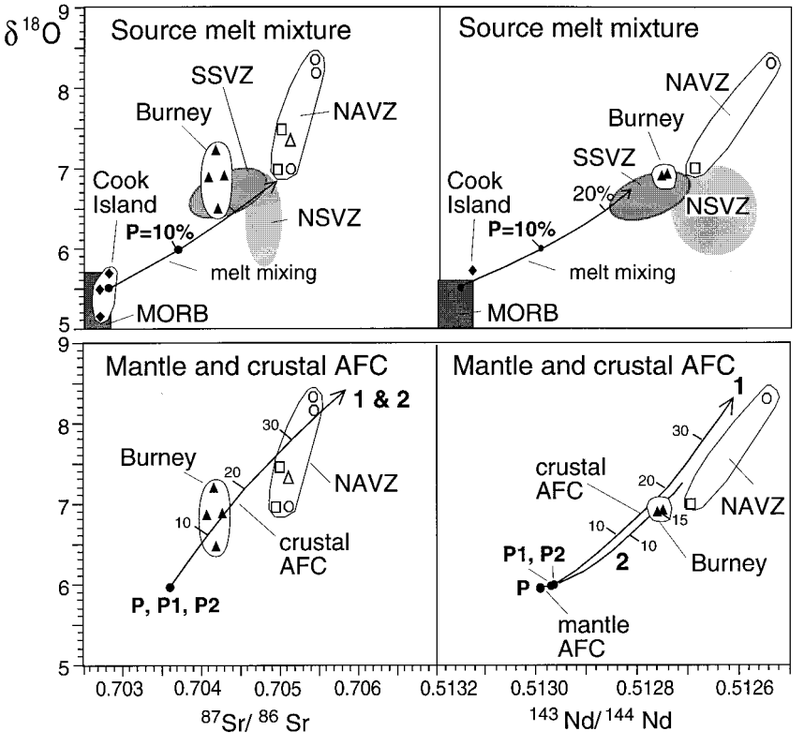

Fig. 10 $\delta^{18}0$ versus $^{87}Sr/^{86}Sr$ and versus $^{143}Nd/^{144}Nd$ for samples from volcanoes of the Andean AVZ. Locations and data sources for other fields (*MORB, low-K SSVZ, NSVZ*) are from Figs. 4, 5 and 8. The upper panels show curves for mixing of partial melt of MORB (10% partial melting) with partial melt of subducted sediment (15% partial melt). Point *P*, which represents 10% of sediment partial melt mixed with 90% of MORB partial melt (Table 4), is the starting parental melt for models of AVZ adakites as discussed in the text. Lower panels illustrate curves for mantle followed by crustal AFC: P1 and P2 are parental melt composition P modified by 120% and 150% mantle AFC (r=1) and curves 1 and 2 are these compositions modified by crustal AFC (r=0.5; Table 4)

Cook Island

Among the AVZ volcanoes, and arc volcanoes from a global perspective, Cook Island andesites are extraordinary in their MORB-like isotopic composition and certain MORB-like trace-element ratios. Ba/La (<5) is significantly lower than typical arc magmas, for which dehydration of subducted oceanic crust and contamination of the sub-arc mantle by alkali and alkaline-earth-element-rich hydrous fluids is considered an important petrogenetic process (Kay 1980). We have previously shown that a model of 4% partial melting of MORB converted to eclogite reproduces many of the trace-element features of the Cook Island andesites, and on this basis suggested direct partial melting of subducted MORB as the source for these andesites (Stern et al. 1984; Futa and Stern 1988). Here we address problems with other alternatives and refine this model.

Myers and Frost (1994) proposed that isotopically similar adakitic andesites from Adak Island might have obtained their unique composition by interaction among more typical calc-alkaline magmas in the magmatic conduits of the Adak volcanic center. Yogodzinski et al. (1995) also presented a model in which silicic melts from the subducted slab interact with basaltic melts in the mantle wedge to produce adakitic andesites. However, in the case of Cook Island, no evidence for a complex system involving basaltic magmas exists, as the volcano consists solely of adakitic andesites. No basalts occur here or anywhere else in the Andean AVZ.

Derivation by partial melting of MORB is more reasonable. The low Yb and Y of Cook Island andesites, which are significantly lower than MORB, and their high Sr, with both positive Sr and Eu anomalies, suggests that partial melting of MORB occurs with garnet, but without plagioclase, in the residue. An important question is; where in the crust-mantle section below the Cook Island volcano is this garnet-amphibolite or eclogitic MORB located? One possibility is in the lower crust, since MOR basalts were emplaced in the southernmost Andes during the formation of the Rocas Verdes back-arc basin in the Cretaceous (Stern 1980, 1991). However, it is unlikely that MORB in the crust has been transformed to garnet-amphibolite or eclogite, as there is no evidence for crustal thickness >35 km below the southern Andes. Also, experimentally determined compositions of hydrous melts of garnet-amphibolite and eclogite generally have lower MgO content and Mg# than Cook Island andesites (Fig. 4). If such melts were to form in the subducted slab, they could increase their Mg# by interaction with peridotite as they rose through the overlying mantle wedge (Keleman 1990, 1995; Keleman et al. 1993). This is not possible for melts formed in the lower crust.

In this convergent plate boundary environment, it is more probable that the MORB source for the Cook Island andesites is the subducted Antarctic plate oceanic crust. Peacock et al. (1994) have shown that because of the young age and slow rates of subduction below the southern Andes, the slab will reach higher temperatures at shallower depths than in typical subduction zones. In the case of Cook Island, the fact that it is located well to the

east of the trench in the direction of convergence implies a longer period of time for subducted oceanic crust to arrive below the volcano, and thus a higher temperature for the slab below this volcano. Peacock et al. (1994) identified the Andean AVZ as one of the few global arc segments where temperatures might reach the melting point of eclogite in the presence of H_2O. The presence of amphibole in the Cook Island andesites implies at least a small amount of water in the source.

Subducted oceanic crust normally would be expected to include altered MORB and sediment, as well as fresh MORB, but based on the isotopic and trace-element data, only the latter appears to have participated in the generation of the Cook Island andesites. As discussed below, subducted sediment may make a significant contribution to the adakitic magmas erupted from other AVZ volcanoes. However, Cook Island is located both further from the trench in the direction of plate convergence, as well as in a region of more oblique subduction angle, than other volcanoes in the AVZ. This may influence the extent to which different materials are either subducted or underplated. Among other adakites world-wide, those from both Cerro Pampa, Argentina (Kay et al. 1993), and the western Aleutians (Yogodzinski et al. 1995), have isotopic compositions that indicate little involvement of subducted sediment and altered oceanic crust, and both also occur either relatively far from the trench or in an area of oblique subduction.

The REE/HFSE ratios of the Cook Island andesites are higher than MORB and similar to typical arc magmas. The explanation normally invoked to explain similar high REE/HFSE in more typical arc magmas, enrichment of the mantle source region by hydrous fluids, can be ruled out for Cook Island andesites because of their MORB-like Ba/La ratios. High REE/HFSE ratios may result from refractory residual phases retaining HFSE, such as rutile, which might be expected for low degrees of partial melting of eclogitic MORB (Rapp et al. 1991; Ayers and Watson 1991; Keleman et al., 1993). Yogodzinski et al. (1995) have shown that the presence of 1% rutile in an eclogitic MORB source can produce the amount of Ta depletion, relative to light-rare-earth elements, observed in both western Aleutian and Cook Island adakites. Also Rb, Ba and K are lower in Cook Island andesites than predicted for 4% melting of N-MORB (Stern et al. 1984). This suggests a small proportion of other residual phase containing these elements, such as mica, amphibole or K-feldpar.

Although the simple eclogite-melt trace-element distribution pattern and MORB-like isotopic composition of Cook Island andesites are consistent with the derivation of these magmas by partial melting of subducted MORB, their high Mg# (Fig. 4) and Ni and Cr contents may result from interaction of these slab-melts with mantle peridotite as they rise through the overlying mantle wedge, as has been suggested for bajaites (Rogers et al. 1985) and other adakites including the type adakite from Adak Island (Kay 1978) and those from Cerro Pampa, Argentina (Kay et al. 1993). Since the mantle wedge is expected to be hotter than either the slab or any slab-melts, it is hard to imagine how such interaction would not occur (Kelemen et al. 1993). High Mg# and Cr/(Cr + Al) clinopyroxene cores in Cook Island andesites (Figs. 2, 3) may be relic xenocrysts from such interaction. However, Cook Island adakites do not have either the very high MgO, Ni and Cr observed in bajaites (Rogers et al. 1985), nor olivine, suggesting that such interaction must have been limited. Also, Cook Island andesites are isotopically distinct from all the Patagonian plateau alkali basalts and included mantle xenoliths which are considered representative of the southern South American lithosphere (Figs. 8, 9). Although the low Sr, Nd and Pb concentration of mantle lithosphere would make limited amounts of mantle contamination difficult to detect, large amounts of such contamination can be ruled out by these isotopic considerations.

Different possible processes have been proposed for the interaction of hydrous slab-derived melts with the overlying maltle wedge, including fluxing of diapiric uprise and decompression melting of the mantle resulting in mixing of slab and mantle derived melts (Yogodzinski et al. 1995), and slab-melt/peridotite reaction and hybridization (Keleman 1990, 1995; Keleman et al. 1993). We prefer slab-melt/peridotite reaction to explain the high Mg# of Cook Island andesites, since there is no direct evidence for mantle-derived basaltic magmas in the AVZ. Physically slab-melt/peridotite interaction involves the reaction of mantle olivine and pyroxenes with relatively silica-rich hydrous melts to produce new minerals (amphibole, pyroxenes, olivine and/or garnet) and hybridized melts (Sekine and Wyllie 1983; Caroll and Wyllie 1989; Keleman 1990, 1995). Keleman (1990, 1995) has suggested that heating of hydrous slab-derived melts ascending through the mantle wedge, due either to the inverted temperature gradient in the wedge (Davis and Stevenson 1992) or to heating resulting from isenthalpic ascent (Baker et al. 1994), provides substantial thermal energy for peridotite dissolution. He concluded that a slab-melt formed at 900°C and heated to 1,200°C has the thermal energy to dissolve an equal weight of peridotite. We have calculated a simple AFC model for a hypothetical slab-melt composition equal to the average of all experimentally determined high-pressure (1–3 GPa), hydrous partial melts of basalts (Fig. 4). This model involves bulk mantle assimilation combined with crystallization of amphibole and clinopyroxenes, the phenocrysts ocurring in Cook Island andesites, with mantle mass-assimilation greater ($r = 2$; DePaolo 1981) than the amount of fractionation, reflecting a relatively hot mantle (Keleman 1990, 1995). This model suggests that dissolution of only between 10–20% peridotite is required to raise the Mg# of a slab-melt to that of the Cook Island andesites (Fig. 4).

Cook Island adakites, as well as many other adakites world-wide, have high CaO contents and CaO/Na_2O ratios compared to typical calc-alkaline andesites. These resemble experimentally determined slab-melts of tonalitic ($CaO/Na_2O > 1$) rather than trondhjemitic

Table 2 Calculated parental melts which can yield Cook Island andesites by assimilation of 10% mantle-mass combined with fractionation of amphibole and clinopyroxene, and published high pressure experimental partial melt of basalts

	Cook	Primitive Mantle	Fractionated minerals:			COOK Parent 1 Mantle assimilation=10%	COOK Parent 2	COOK Parent 3	Trondhjemitic			Tonalitic			
			Cpx 20%	Hbl 80%	Sum 100%	r=1	r=2	r=8	9#	10#	11#	12#	13#	14#	15#
SiO_2	60.23	45.96	51.02	45.03	46.23	60.26	61.00	61.60	67.66	70.10	65.93	62.47	62.30	63.11	61.70
TiO_2	0.78	0.18	0.63	2.08	1.79	0.94	0.90	0.86	0.61	0.94	1.31	0.42	–	0.73	0.80
Al_2O_3	18.07	4.06	4.70	11.61	10.23	18.69	19.13	19.50	17.45	15.54	17.55	20.93	22.70	16.50	19.50
FeO	3.56	7.54	5.89	9.06	8.43	3.65	3.40	3.19	1.89	1.78	3.15	4.93	2.30	5.26	5.60
MnO	0.07	0.20	0.12	0.07	0.08	0.06	0.06	0.06	–	0.07	0.12	0.10	–	0.10	0.06
MgO	4.05	37.78	14.42	15.74	15.48	1.82	1.10	0.51	0.62	0.43	1.02	1.33	0.20	2.48	1.50
CaO	7.97	3.21	22.48	11.29	13.53	9.00	8.76	8.57	1.61	1.89	1.47	8.53	7.90	5.72	6.40
Na_2O	4.37	0.33	0.73	2.91	2.47	4.58	4.70	4.79	4.89	5.44	6.72	1.13	3.60	3.42	3.40
K_2O	0.58	0.00	0.00	0.13	0.10	0.59	0.62	0.64	5.29	3.82	2.55	0.28	0.70	–	1.30
P_2O_5	0.31	0.00	0.00	0.00	0.00	0.31	0.33	0.34	–	–	–	–	–	–	–
Total	100.00	99.26	100.00	97.91	98.33	100.00	100.00	100.00	100.02	100.01	99.82	100.12	99.70	97.32	100.26
Mg# (Fe tot)	67.0	89.9	81.4	75.6	Bulk D	47.1	36.6	21.8	36.9	30.1	36.6	32.5	13.4	45.7	32.3
Rb	3.00	0.54	0.080	0.100	0.096	2.98	3.11	3.21	9=Sen & Dunn (1994); 2 GPa, run B16						
Ba	177	6	0.060	0.070	0.068	177	186	192	10=Rapp et al. (1991); 3.2 GPa, Rock #2, 1075° C						
Th	4.40	0.08	0.050	0.050	0.050	4.41	4.60	4.78	11=Rapp et al. (1991); 3.2 GPa, Rock #1, 1100° C						
U	1.30	0.02	0.015	0.040	0.035	1.30	1.37	1.41	12=Wolf and Wyllie (1994); 1 GPa, 138SD:3						
K	4981	258	0.020	0.100	0.084	4997	5226	5396	13=Stern and Wyllie (1978); 3 GPa, 5% H_2O, 900° C						
Ta	0.61	0.04	0.240	0.210	0.216	0.62	0.64	0.65	14=Yogodzinski et al. (1995); smlt2						
La	35.30	0.614	0.600	0.050	0.160	35.80	37.30	38.4	15=Johannes and Wolke (1994); 1 GPa, 900° C						
Ce	75.70	1.601	0.900	0.060	0.228	77.30	80.20	82.4	Primitive mantle=Hofmann (1988)						
Nd	28.10	1.189	0.400	1.200	1.040	31.00	30.90	30.8	D_{Cpx} and D_{Hbl} from Brennan et al. (1994),						
Sr	2003	18	0.100	0.200	0.180	2038	2120	2181	Johnson (1994), Martin (1993), Sen and Dunn						
Zr	122	10	0.300	0.250	0.260	124	129	132	(1994) and Schnetger (1993)						
Y	6.00	3.90	0.800	2.500	2.160	7.01	6.58	6.3							
Yb	0.990	0.414	0.900	2.200	1.940	1.160	1.100	1.06							
Lu	0.040	0.064	0.900	3.000	2.580	0.040	0.042	0.042							
Cr	65	1200	30.000	30.000	30.000	550	20	0							
$^{87}Sr/^{86}Sr$	0.70280	0.7036				0.70280	0.70280	0.70280							
$^{143}Nd/^{144}Nd$	0.51315	0.5128				0.51315	0.51315	0.51315							
$\delta^{18}O$	5.5	6.5				5.5	5.5	5.45							
100/Nd	3.56	84.09				3.23	3.24	3.25							
1000/Sr	0.50	54.95				0.49	0.47	0.46							
Sr/Y	334	4.7				291	322	346							

($CaO/Na_2O<1$) composition (Table 2). Yogodzinski et al. (1995) concluded that transforming low CaO/Na_2O trondhjemitic slab-melts into high CaO/Na_2O adakitic andesites would require extensive assimilation of mantle peridotite (roughly twice the mass of the original melt to get enough CaO from garnet and clinopyroxene into the melt), followed by equally extensive fractionation of olivine and orthopyroxene (roughly 50% of the mass of this mixture to get the MgO and FeO out). Both the absence of either olivine or orthopyroxene in the Cook Island andesites, and the isotopic differences between these andesites and samples of the mantle lithosphere below Southern South America, rule out such extensive interaction. Also, such extensive assimilation and fractionation would not preserve the simple eclogite-melt trace-element distribution pattern observed in the Cook Island andesites.

If the original slab-melt has higher CaO/Na_2O, then significantly less mantle assimilation is required to produce an adakitic andesite. For instance, Yogodzinski et al. (1995) proposed 26% assimilation of mantle peridotite, followed by 34% orthopyroxene fractionation, to produce the major-element composition of western Aleutians adakitic andesites from a tonalitic slab-melt. However, only clinopyroxene and amphibole phenocrysts are observed in Cook Island andesites. We have back-calculated possible parental slab-melts for Cook Island andesites with AFC models (DePaolo 1981) involving fractionation of these phases in their observed proportions (80% amphibole and 20% clinopyroxene), and variable proportions of mantle assimilation ranging from equal ($r = 1$) to greater ($r = 2$ and $r = 8$) than the amount of fractionation, reflecting a relatively hot mantle wedge (Keleman 1990, 1995). Our calculated parental slab-melts (Table 2), from which Cook Island andesites can be derived by assimilation of 10% mantle peridotite, are high CaO/Na_2O magmas with between 2.0 and 0.5 wt% MgO; reasonably similar to suggested tonalitic slab-melts. With up to 10% assimilation of mantle, the trace-element concentrations calculated for these parental magmas of Cook Island andesites (Table 2) are still consistent with models of derivation by 2–3% partial melting of eclogitic MORB. Greater than 10% mantle mass assimilation would produce parental magmas requiring $\leq$2% MORB melting, which is below the lower limit for the segregation of a magma suggested by Wyllie and Wolf (1993).

In summary, we propose a simple slab-melt origin for Cook Island andesite, followed by limited ($\leq$10% mass assimilation) interaction in the overlying mantle. Rapid rise through both the mantle and the upper crust, perhaps along pathways related to the strike-slip plate boundary between the South American and Scotia plates (Fig. 1), is suggested by this limited extent of interaction with the mantle, and by the lack of plagioclase phenocrysts in these andesites. Also their MORB-like O- and Pb-isotopic compositions, combined with their low Pb concentration, preclude crustal contamination.

Other AVZ volcanoes

The other volcanoes of the AVZ do not have the distinctive MORB-like isotopic signature of Cook Island. However, they all have low HREE and Y and high Sr/Y which suggests garnet in their source, and like Cook Island they occur in a region of relatively thin crust (<35 km) within which plagioclase rather than garnet is likely to be stable. If the thermal conditions for melting of subducted MORB occur below Cook Island, it seems likely that they may also occur below the other AVZ volcanoes, under which even younger oceanic crust is being subducted (Fig. 1). However, it is clear that other material such as continental crust, subducted sediment, and/or the mantle wedge must have participated in the generation of magmas erupted from these volcanoes to create the observed trace-element ratios (Fig. 7) and isotopic (Figs. 8–10) variations. We discuss below models for the generation of the other AVZ volcanoes involving these other materials, first individually, and then together.

From south to north, the volcanoes of the AVZ define a trend of decreasing MgO (Fig. 4) and Sr content and $^{143}Nd/^{144}Nd$ ratios (Fig. 8), and increasing SiO_2, K_2O (Fig. 5), $^{87}Sr/^{86}Sr$ (Fig. 8) and $\delta^{18}O$ (Fig. 10). These relations, as well as the petrologic features of increased modal phenocryst and xenocryst proportions, suggest a northward increase in the importance of combined fractional crystallization and crustal assimilation (AFC) in shallow level magma chambers (Stern et al. 1984). However, the relatively high Mg# (Fig. 4) and Sr, as well as low Y b and Y (Fig. 6) of all the AVZ volcanoes rule out typical Andean basalts as possible parental magmas (Stern et al. 1984). A crustal AFC model involving a parental magma similar to the Cook Island andesite, with $r = 0.5$, can produce the observed Sr versus $^{87}Sr/^{86}Sr$ relations by 30% fractionation for Burney and 50% for the NAVZ. However, this model fails to produce many other significant geochemical characteristics of these AVZ centers compared to Cook Island, in particular the low LIL and LREE of Burney adakites. Crustal AFC may be important in the generation of all the AVZ centers north of Cook Island, but can not be the only processes involved in creating the variations observed among these centers.

Subduction of both pelagic and terrigenous sediment, and/or subduction erosion of continental crust, are also likely processes by which greater proportions of these high $^{87}Sr/^{86}Sr$ and $\delta^{18}O$ materials might have been incorporated in the AVZ magmas erupted from the volcanoes north of Cook Island. Also, AVZ adakites have Pb-isotopic compositions which occur along a mixing line between MORB and Chile Trench sediment (Fig. 9). However a model involving mixing of MORB melts with melts derived from subducted sediments (Figs. 10, 11), cannot by itself produce the isotopic variations observed among the AVZ magmas. Specifically, the amount of subducted sediment required to produce the $^{87}Sr/^{86}Sr$ of Burney and NAVZ andesites and dacites (Fig. 11a) is much less than that required to produce their $\delta^{18}O$ (Fig. 10) and $^{143}Nd/^{144}Nd$ (Fig. 11b) values.

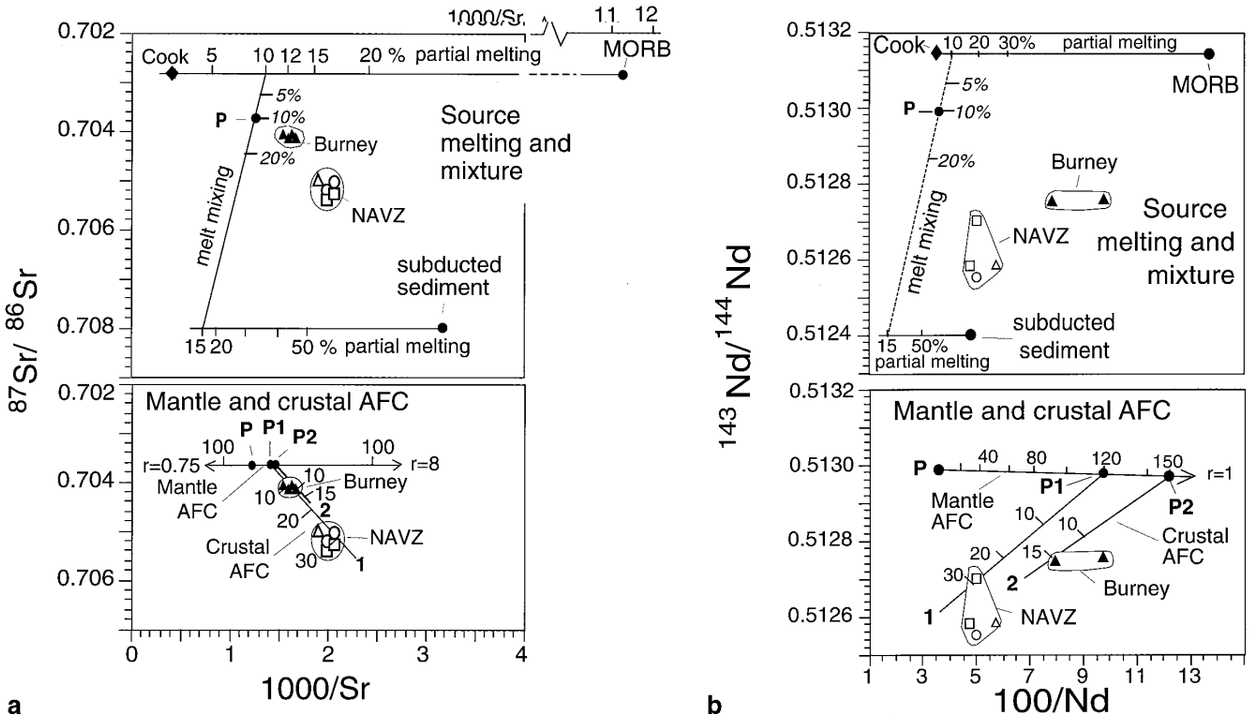

Fig. 11 a, b 1000/Sr versus $^{87}Sr/^{86}Sr$ and 100/Nd versus $^{143}Nd/^{144}Nd$ for slab-melts followed by mantle and crustal AFC processes as described in the text. Trends for mantle AFC with r = 0.75 (*arrow* to high Sr) and r = 8 (*arrow* to low Sr) are illustrated for 1000/Sr versus $^{87}Sr/^{86}Sr$

The genesis of most typical arc magmas is generally attributed to melting of the mantle wedge fluxed by addition of small (<2%) amounts of slab-derived fluids (Pearce and Parkinson 1993). Slab-melts rising into the hot mantle wedge are also likely to interact with this mantle peridotite. Interaction of slab-melts with mantle peridotite may lower incompatible LIL and LRE element concentrations relative to more compatible trace-elements (Keleman et al. 1993). Although variations in the extent of interaction with the mantle wedge alone cannot explain the isotopic variations observed among the AVZ adakites, interaction of slab-derived melts within the mantle wedge could potentially produce magmas with the low LIL and LREE of Burney adakites. MgO-rich olivine and clinopyroxene xenocrysts in Burney andesites (Figs. 2, 3) might be relics of such interaction, although the general lack of olivine in all AVZ adakites indicates that such interactions were limited, and as for Cook Island andesites, other AVZ adakites have not equilibrated with mantle peridotite.

We have attempted to model Burney and NAVZ adakites by multi-stage processes of slab (MORB + sediment) melting, followed by interaction of these melts with the mantle wedge, and subsequently crustal AFC (Figs. 10–13; Table 4). The composition of N-MORB, primitive mantle, subducted sediment and continental crust, and the distribution coefficients used in these models are listed in Table 3. The subducted sediment is from ODP Leg 141 in the Chile Trench (Behrmann and Kilian 1995), and the continental crust is a mixture of average southern South American metamorphic basement (S-type) and plutonic rocks (I-type; Behrmann and Kilian 1995). In order to model the melting of subducted MORB, we calculated a bulk distribution coefficient D_{MORB} (Table 3) by assuming that the Cook Island parental magma #2 (Table 2) was generated by 2.5% melting of N-MORB. In order to model melting of subducted sediment, we caluclated the bulk distribution coefficient $D_{Sediment}$ by adding 20% biotite to D_{MORB}. Bulk distribution coefficients for the mineral assemblages involved in mantle and crustal AFC processes were calculated based on published distribution coefficients for these minerals.

We presume that if MORB melts, so do subducted sediments (Nichols et al. 1994). We varied the percentage of partial melting of MORB and subducted sediment independently, and mixed the resulting melts together in different proportions, to produce one best parental composition (*P*; Figs. 10–13; Table 4), which can yield both Burney and NAVZ magmas by subsequent mantle and crustal AFC. Parental composition *P* corresponds to a mixture of 10% sediment partial melt (15% partial melting) with 90% MORB partial melt (10% partial melting). Lower degrees of partial melting of either sediment or MORB resulted in melts with unrealistically high incompatible element concentrations, while higher degrees of partial melting of sediment decreased Sr concentrations so that the resulting mixtures with MORB melts have unacceptably high $\delta^{18}O$ at relatively low $^{87}Sr/^{86}Sr$. Mixing higher percentages of sediment partial melts

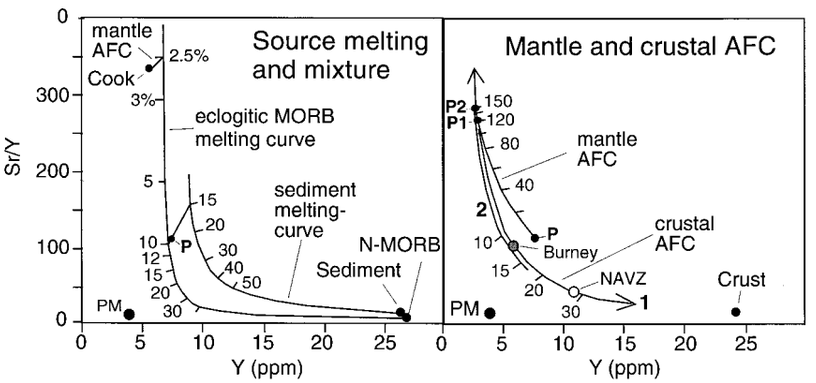

Fig. 12 Sr/Y versus Y for slab-melts followed by mantle and crustal AFC processes as described in the text

with MORB melts results in compositions with $^{87}Sr/^{86}Sr$ equal to or greater than Burney (Figs. 10, 11), which precludes subsequent crustal AFC, but at the same time does not produce the required low $^{143}Nd/^{144}Nd$ of Burney magmas. Composition *P* is essentially the maximum amount of sediment that may be incorporated in the parental slab-melt and still allow a specific amount of subsequent crustal AFC to produce both the $^{87}Sr/^{86}Sr$ and $^{143}Nd/^{144}Nd$ of the Burney magmas. With this same parental slab-melt composition, NAVZ magmas can be modeled with greater amounts of crustal AFC. Alternatively, more subducted sediment could be incorporated in the slab-melt parental magmas for NAVZ volcanoes, but the model presented here attempts to explain both Burney and NAVZ magmas from similar parental slab-melt.

The resultant parental slab-melt *P* has both higher Sr and higher Nd concentrations than either Burney or NAVZ magmas (Fig. 11; Table 4). Although Sr decreases, Nd concentration increases during crustal AFC. For this reason, interaction of slab-melts with mantle peridotite must be an important process below these AVZ volcanoes in order to lower Nd concentrations of these slab-melts prior to crustal AFC. We have modeled this interaction assuming mantle assimilation combined with fractional crystallization of the evolving magmas. We calculated mantle AFC models with variable mass-assimilation/fractionation ratios (r = 0.75, r = 1 and r = 8), using the mafic phenocryst phases observed in AVZ magmas (amphibole, clinopyroxene, orthopyroxene and Ti-magnetite) as fractionating phases. All these different r-values result in decreasing Nd with increasing mantle mass-assimilation. However, high mass-assimilation/fractionation ratios (r = 8 as well as bulk mantle assimilation), while physically possible in a hot mantle wedge (Keleman et al. 1993), result as well in an unsuitable decrease of Sr (Fig. 11a) and other LIL element concentrations. In contrast, low mass-assimilation/fractionation ratios (r = 0.75) result in an unsuitable increases in Sr (Fig. 11a) and other LIL element concentrations. For r = 1, Sr and LIL concentrations remain nearly constant as Nd, Y and HREE decrease (Figs. 11–13).

For mantle AFC with r=1, 120% and 150% mantle mass-assimilation by parental slab-melt *P* produce compositions *P1* and *P2*, respectively (Figs. 10–13; Table 4). From composition *P1*, NAVZ magmas may be modeled by 20–30% crustal AFC, using the commonly employed value r = 0.5 (DePaolo 1981). From composition *P2*, Burney magmas may be modeled by 10–15% crustal AFC. The greater amount of mantle mass-assimilation required to produce Burney compared to NAVZ magmas reflects the significantly lower LIL and LREE of Burney adakites. The smaller proportion of crustal AFC required

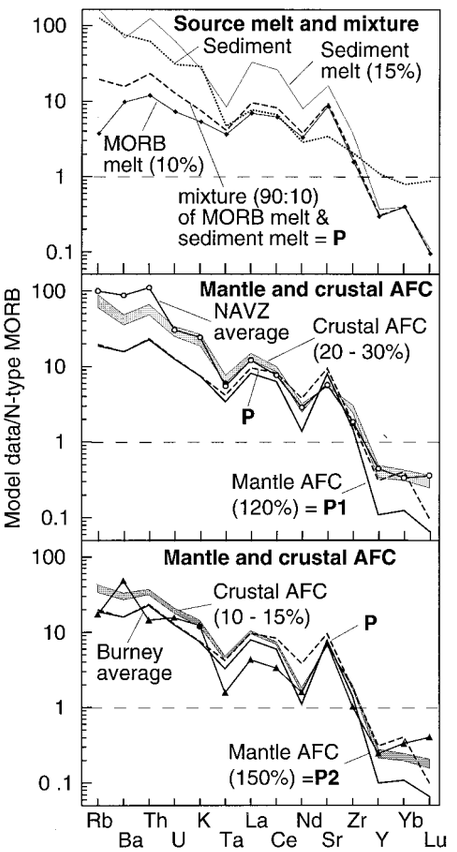

Fig. 13 Spider diagrams showing multi-element fit for the best model of slab melting followed by mantle and crustal AFC as descibed in the text

Table 3 Compositions of materials and distribution coefficients used in slab melting followed by mantle and crustal AFC for adakites[a]

	N-MORB	Primitive Mantle	ODP 141 sediments	S-type crust	I-type crust	Crustal mixture (50:50)	$D_{biotite}$	D_{MORB}	$D_{Sediment}$	Ds for mantle AFC	Ds for crustal AFC
Rb	0.56	0.54	74	101	74	87	3.00	0.17	0.74	0.083	0.032
Ba	6.3	6	445	482	489	485	5.60	0.01	1.13	0.060	0.111
Th	0.12	0.08	6	8.4	7.2	7.8	2.00	0.002	0.40	0.053	0.020
U	0.047	0.02	1.8	1.6	2	1.75	2.00	0.01	0.41	0.042	0.020
K	600	258	17000	13695	21266	17481	5.00	0.10	1.08	0.072	0.061
Ta	0.132	0.035	0.6	1	1.1	1.05	1.60	0.20	0.48	0.243	0.010
La	2.5	0.6	19	24.6	24	24.3	0.30	0.05	0.10	0.164	0.143
Ce	7.5	1.6	49	52.9	45.4	49.2	0.34	0.07	0.12	0.253	0.141
Nd	7.3	1.2	21	28.8	18.6	23.6	0.32	0.22	0.24	0.910	0.140
Sr	90	18	305	173	267	220	0.30	0.02	0.08	0.156	1.025
Zr	74	10	149	180	160	170	0.08	0.60	0.50	0.236	0.073
Y	28	3.9	27	27	21	24	0.10	4.10	3.30	1.875	0.010
Yb	3.05	0.41	2.4	1.96	1.94	1.95	0.10	2.70	2.18	1.682	0.295
Lu	0.455	0.064	0.4	0.27	0.3	0.26	0.10	11.60	9.30	2.208	0.295
$^{87}Sr/^{86}Sr$	0.7025	0.7036	0.708	0.723	0.707	0.715				(66% Hbl,	(50% Pl,
$^{143}Nd/^{144}Nd$	0.51315	0.5128	0.5124	0.512	0.5125	0.5123				20% Cpx,	25% Cpx,
$\delta^{18}O$	5.5	6.5	10	14	10	12				10% Cpx,	25% Cpx,
										4% Ti-Mt)	

[a] N-MORB from Sun and McDonough (1989); primitive mantle from Hofmann (1988); D_{MORB} (calculated as described in the text), $D_{Sediment}$=(80% D_{MORB}+20% $D_{biotite}$); $D_{biotite}$, D_{Hbl}, D_{Cpx}, $D_{Ti\text{-}Mt}$ from references in Table 2; ODP Leg 141 sediments, S-type (metamorphic basement) and I-type (Patagonian Batholith) crust from Behrmann and Kilian (1995) and unpublished data

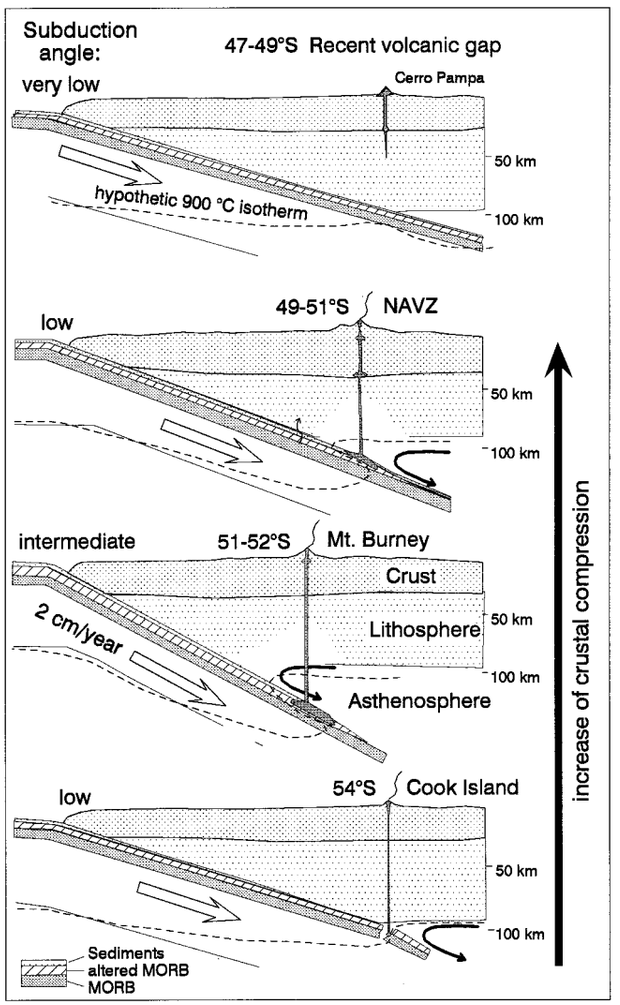

Fig. 14 Schematic cross-sections below the different volcanic centers, from north-to-south, of the Andean AVZ. The angle of subduction is surmised to increase southwards from near the Chile Rise-Trench triple junction to below Burney, and than decrease again as convergence direction becomes more oblique. The extent of crustal compression is surmised to increase northwards as the angle of subduction becomes more orthogonal. These factors affect the extent of mantle and crustal AFC processes as descibed in the text

to produce the Burney magmas reflects the more primitive isotopic composition of these magmas.

Conclusions

Although considerable uncertainties relate to both the composition of the different components and the equilibrium bulk assimilation AFC processes, particularly for slab-melt/mantle peridotite interaction, employed in our multi-stage, four-component (MORB, subducted sediment, mantle wedge, crust) model, this model gives a reasonable fit to the observed trace-element and isotopic compositions of AVZ andesites, specifically Sr, Nd and Y contents and O, Sr and Nd isotopic compositions (Figs. 10–13; Table 4). The mass contribution from the subducted slab in this model is high compared to typical arc magmas. This is consistent with geothermal models which suggest melting of the young and slowly subducting slab in this region of the Andean arc (Peacock et al. 1994). Our model also involves a significant amount of subducted sediment in the generation of all the AVZ adakites except those from Cook Island.

The proportions of the different source materials involved in the genesis of AVZ magmas vary significantly from north-to-south. A basis for rationalizing these vari-

Table 4 Calculated trace-element and isotopic compositions of the slab-melt parental magmas and this magma modified first by mantle and subsequently crustal AFC (*Ma* mass assimilated, *Mc* mass crystallized)

	Partial melting[a]		90% MORB & 10% sediment melt	AFC Modelling			Average NAVZ	AFC Modelling			Average Burney
	MORB 10% Partial melt	Sediment 15% Partial melt	P	Mantle Ma=120% Mc=120% P-1	Crust Ma=20% Mc=40%	Crust Ma=30% Mc=60%		Mantle Ma=150% Mc=150% P-2	Crust Ma=10% Mc=20%	Crust Ma=15% Mc=30%	
Rb	2.2	95.4	11.5	11.1	34.8	51.3	59.0	10.9	21.6	24.8	10.0
Ba	58	401	92	93	217	298	514	93	150	193	278
Th	1.2	12.2	2.3	2.2	4.9	6.4	10.9	2.2	3.3	4.0	1.4
U	0.4	3.6	0.8	0.7	1.3	1.8	1.8	0.7	1.0	1.2	0.9
K	3158	15918	4434	4365	9627	13509	17198	4348	6702	8074	7222
Ta	0.47	1.08	0.53	0.43	0.78	1.02	0.70	0.41	0.57	0.66	0.20
La	17.2	80.9	23.6	20.1	27.8	32.8	29.8	19.3	22.8	24.8	10.4
Ce	46.0	191.9	60.6	46.4	60.1	68.6	56.4	43.5	49.8	53.2	24.4
Nd	24.5	59.3	28.0	10.3	17.0	21.5	21.0	8.1	11.1	12.8	11.6
Sr	765	1423	831	709	541	466	500	682	600	560	624
Zr	116	261	130	108	169	211	135	104	131	146	74
Y	7.4	9.1	7.6	2.7	8.4	12.1	10.9	2.4	5.1	6.6	6.0
Yb	1.21	1.20	1.20	0.37	0.85	1.15	1.00	0.32	0.55	0.66	0.99
Lu	0.04	0.05	0.04	0.03	0.10	0.14	0.16	0.03	0.06	0.08	0.18
Cr		20	20	42	2	1	3	42	6	3	3
$^{87}Sr/^{86}Sr$	0.70280	0.70800	0.70369	0.70369	0.70455	0.70515	0.70520	0.70369	0.70409	0.70433	0.70420
$^{143}Nd/^{144}Nd$	0.51315	0.51240	0.51299	0.51297	0.75128	0.51268	0.51262	0.51297	0.51281	0.51276	0.51275
$\delta^{18}O$	5.50	10.00	5.98	5.99	7.20	7.80	7.70	6.00	6.60	6.90	6.80
Sr/Y	104	156	110	265	64	39	46	281	118	85	104
1000/Sr	1.31	0.70	1.20	1.41	1.85	2.15	2.00	1.47	1.67	1.78	1.60
100/Nd	4.1	1.7	3.6	9.7	5.9	4.7	4.8	12.3	9.0	7.8	8.6

[a] Melting of MORB and sediment with bulk Ds from Table 3

ations in the tectonic context of the AVZ is provided by the schematic cross-sections in Fig. 14. Just south of the triple junction (46–49°S), a gap in active volcanism occurs in the region where very young oceanic lithosphere is being subducted, presumably at very low angle. Further to the south below the NAVZ (49–51°S), melting of the slab (MORB + sediment) and interaction of these melts with a relatively small mantle wedge, followed by significant crustal AFC, produces the NAVZ adakites. Even further south below Reclus and Burney (51–52°S), the lower LIL and LREE of magmas erupted from these volcanoes suggest greater interaction within the mantle of slab-derived melts. In this region the subducted lithosphere is older and the subduction angle may be greater, so that the mantle wedge may be larger or more actively convecting and thus hotter. On the other hand, crustal AFC process are less significant than below the NAVZ. This may be due to the increasingly oblique nature of subduction as well as the influence of the strike-slip Malvinas/Magallanes fault system (Fig. 1) in providing paths for the relatively rapid rise of sub-crustal magmas at this latitude. Even further south below Cook Island (54°S), oblique subduction, fragmentation of the subducted slab and deep lithospheric faults allow small proportions of MORB melt to rise through both the mantle and crust with only very limited interaction.

Acknowledgements We thank A. Puig and L. Dickenson for providing some samples, and A. Skewes, E. Leonard, R. Fuenzalida, S. Harambour and J. Lobato for logistic support in obtaining others. K. Futa, K. Muehlenbachs, L. Farmer and B. Barreiro provided some of the isotopic data, and H. Meyer was helpful in producing the microprobe data. The final mauscript was improved by comments from T. Dunn, T. Grove and an anonymous reviewer. This research was supported by NSF grants EAR76-03816, EAR80-20791 and EAR83-13884, and German Research Foundation grants Ki-345/1 and Ki-456/1.

References

Ayers JC, Watson EB (1991) Rutile solubility and mobility in supercritical aqueous fluids. Contrib Mineral Petrol 114: 321–330

Baker MB, Grove TL, Price R (l994) Primitive basalts and andesites from the Mt. Shasta region, N. California: products of varying melt fraction and water content. Contrib Mineral Petrol 118: 111–129

Barreiro B (l983) Lead isotopic compositions of South Sandwich Island volcanic rocks and their bearing on magmagenesis in intra-oceanic island arcs. Geochim Cosmochim Act 47: 817–822

Behrmann J, Kilian R (l995) Chemical and isotopic constraints on the origin of Pleistocene to Pliocene trench sediments at the Chile triple junction (abstract). IUGG XXI General Assembly: A450

Brennan JM, Shaw HF, Phinney DL (l994) Experimental determination of trace element partitioning between pargasitic amphibole and hydrous melt. Mineral Mag 58: 121–122

Bruhn RL, Dalziel IWD (1977) Destruction of the Early Cretaceous marginal basin in the Andes of Tierra del Fuego. In: Talwani M, Pitman WC (eds) Island arcs, deep sea trenches, and back-arc basins (Maurice Ewing Series 1) American Geophysical Union, Washington, pp 395–406

Cande SC, Leslie RB (1986) Late Cenozoic tectonics of the Southern Chile Trench. J Geophys Res 91: 471–496

Carroll MR, Wyllie PJ (l989) Experimental phase relations in the system tonalite-peridotite-H_2O at 15 kb: implications for assimilation and differentiation processes near the crust-mantle boundary. J Petrol 30: 1351–1382

Davis JH, Stevenson DJ (l992) Physical model of source region of subduction zone volcanics. J Geophys Res 97: 2037–2070

Defant MJ, Drummond MS (1990) Derivation of some modern arc magmas by melting of young subducted lithosphere. Nature 347: 662–665

Defant MJ, Drummond MS (1993) Mount St. Helens: potential example of partial melting of subducted lithosphere in a volcanic arc. Geology 21: 547–550

Defant MJ, Clark LF, Stewart RH, Drummond MS, de Boer JZ, Maury RC, Bellon H, Jackson TE and Restrepo JF (1991a) Andesite and dacite genesis via contrasting processes: the geology and geochemistry of El Valle Volcano, Panama. Contrib Mineral Petrol 106: 309–324

Defant MJ, Richerson PM, De Boer JZ, Stewart RH, Maury RC, Bellon H, Drummond MS, Feigenson MD, Jackson TE (1991b) Dacite genesis via both slab melting and differentiation: petrogenesis of La Yeguada Volcanic Complex, Panama. J Petrol 32: 1101–1142

DePaolo DJ (1981) Trace element and isotopic effects of combined wall-rock assimilation and fractional crystallization. Earth Planet Sci Lett 53: 189–202

Drummond MS, Defant MJ (1990) A model for trondhjemite-tonalite-dacite genesis and crustal growth via slab melting: Archean to modern comparisons. J Geophys Res 95: 21503–21521

Forsyth DW (1975) Fault plane solution and tectonics of the South Atlantic and Scotia Sea. J Geophys Res 80: 1429–1443

Fuenzalida RP (1974) The Magallanes Fault zone. In: Gonzales-Ferran O (ed) Andean and Antarctic volcanologic problems. Proceedings IAVCEI Intern Volcan Sympos, Santiago, Chile, pp 373–391

Futa K, Stern CR (1988) Sr and Nd isotopic and trace element compositions of Quaternary volcanic centers of the southern Andes. Earth Planet Sci Lett 88: 253–262

Gill JB (1981) Orogenic andesites and plate tectonics. Springer, Berlin Heidelberg New York

Green TH, Ringwood AE (1968) Genesis of calc-alkaline igneous rock suite. Contrib Mineral Petrol 18: 105–162

Harambour SM (l988) Sobre el hallazgo del mitico volcan Reclus, ex Mano del Diablo, Hielo Patagonico Sur, Magallanes, Chile. Rev Geol Chile 15: 173–180

Herron EM, Bruhn R, Winslow M, Chuaqui L (1977) Post Miocene tectonics of the margin of southern Chile. In: Talwani M, Pitman WC (eds) Island arcs, deep sea trenches and back-arc basins (Maurice Ewing Series 1). American Geophysical Union, Washington, pp 273–283

Heusser CJ, Heusser LE, Hauser A (l990) A 12,000 B.P. tephra layer at Bahia Inutil (Tierra del Fuego, Chile). Ans Ins Pat l9: 39–49

Hofmann AW (1988) Chemical differentiation of the Earth: relationship between mantle, continental crust and oceanic crust. Earth Planet Sci Lett 90: 297–314

Johannes W, Wolke C (l994) Bildung von tonalitischen Teilschmelzen - ein Schritt in der Entwicklung der kontinentalen Kruste. Eur J Mineral 6: 126

Johnson KTM (l994) Experimental cpx/and garnet/melt partitioning of REE and other trace elements at high pressures: petrologic implications. Mineral Mag 58: 454–455

Kay RW (1978) Aleutian magnesium andesites: melts from subducted Pacific oceanic crust. J Volcanol Geotherm Res 4: 117–132

Kay RW (1980) Volcanic arc magmas: implications of a melting-mixing model for element recycling in the crust upper mantle system. J Geol 88: 497–522

Kay SM, Ramos VA, Marquez M (1993) Evidence in Cerro Pampa volcanic rocks for slab-melting prior to ridge-trench collision in Southern South America. J Geol 101: 703–714

Keleman PB (l990) Reaction between ultramafic rock and fractionated basaltic magma. I. Phase relations, the origin of calc-alkaline magma series, and the formation of discordant dunite. J Petrol 31: 51–98

Keleman PB (l995) Genesis of high Mg# andesites and the continental crust. Contrib Mineral Petrol 120: 1–19

Keleman PB, Shimizu N, Dunn T (1993) Relative depletion of niobium in some arc magmas and the continental crust: partitioning of K, Nb, La and Ce during melt/rock reaction in the upper mantle. Earth Planet Sci Lett 120: 111–134

Kilian R (l995) Interaction of tonalitic melts with mantle peridotite: evidence from a xenolith of the southern Andes (abstract). IUGG XXI General Assembly: A468-469

Kilian R, Lopez-Escobar L, Lobato J (1991) Quaternary volcanism of the Austral Volcanic Zone of the Andes (49–52°S): geochemistry and petrology. Zentralbl Geol Paläontol Teil 1: 1709–1721

Lopez-Escobar L, Kilian R, Kempton PD, Tagiri M (l993) Petrology and geochemistry of Quaternary rocks from the Southern Volcanic Zone of the Andes between 41°30′ and 46°00′S, Chile. Rev Geol Chile 20: 33–56

Martin H (1993) The mechanisms of petrogenesis of the Archaean continental crust: comparison with modern processes. Lithos 30: 373–388

Martinic M (1988) Actividad volcanica historica en la region de Magallanes. Rev Geol Chile 15: 181–186

Morris P (1995) Slab melting as an explanation of Quaternary volcanism and aseismicity in southwest Japan. Geology 23: 395–398

Muehlenbachs K, Clayton RN (l972) Oxygen isotope studies of fresh and weathered submarine basalts. Can J Earth Sci 9: 172–184

Myers JD, Frost CD (1994) A petrologic re-investigation of the Adak volcanic center, central Aleutian arc, Alaska. J Volcanol Geotherm Res 60: 109–146

Nichols GT, Wyllie PJ, Stern CR (l994) Subduction zone melting of pelagic sediments constrained by melting experiments. Nature 371: 785–788

Peacock SM, Rushmer T, Thompson AL (1994) Partial melting of subducted oceanic crust. Earth Planet Sci Lett 121: 227–244

Pearce JA, Parkinson IJ (1993) Trace element models for mantle melting: application to volcanic arc petrogenesis. In: Prichard HM, Alabaster T, Harris NBW, Neary CR (eds) Magmatic processes and plate tectonics. Geol Soc London Spec Pub 76: 373–403

Peng ZC, Zartman RE, Futa K, Chen DG (l986) Pb-, Sr- and Nd-isotopic systematics and chemical characteristics of Cenozoic basalts, eastern China. Chem Geol 59: 3–33

Puig AG, Herve M, Suarez M, Saunders AD (1984) Calc-alkaline and alkaline Miocene and calc-alkaline recent volcanism in the Southermost Patagonian Cordillera, Chile. J Volcanol Geotherm Res 21: 149–163

Ramos VA, Kay SM (l992) Southern Patagonian plateau basalts and deformation: backarc testimony of ridge collision. Tectonophysics 205: 261–282

Rapp RP, Watson EB, Miller CF (1991) Partial melting of amphibolite/eclogite and the origin of Archean trondhjemites and tonalites. Precambrian Res 51: 1–25

Rogers G, Saunders AD, Terrell DJ, Verma SP, Marriner GF (1985) Geochemistry of Holocene volcanic rocks associated with ridge subduction in Baja, California, Mexico. Nature 315: 389–392

Schnetger B (l993) Partial melting during the evolution of the amphibolite- to granulite gneisses of the Ivrea Zone, northern Italy. Chem Geol 113: 71–101

Sekine T, Wyllie PJ (l983) Experimentasl similation of mantle hybridization in subduction zones. J Geol 91: 511–528

Selverstone J, Stern CR (l983) Petrochemistry and recrystallization history of granulite xenoliths from the Pali-Aike volcanic field, Chile. Am Mineral 68: 1102–1112

Sen C, Dunn T (1994) Dehydration melting of a basaltic composition amphibolite at 1.5 and 2.0 GPa: implications for the origin of adakites. Contrib Mineral Petrol 117: 394–409

Stern CR (1974) Melting products of olivine tholeiite basalt in subduction zones. Geology 2: 227–230.

Stern CR (1980) Chemistry of Chilean ophiolites: evidence for the compositional evolution of the mantle source of back-arc basin basalts. J Geophys Res 85: 955–966

Stern CR (1990) Tephrochronology of southermost Patagonia. National Geograph Res 6: 110–126

Stern CR (l991) Isotopic composition of late Jurassic and early Cretaceous mafic igneous rocks from the southernmost Andes: implications for sub-Andean mantle. Rev Geol Chile 18: 15–23

Stern CR, Wyllie PJ (1978) Phase compositions through crystallization intervals in basalt-andesite-H_2O at 30 kbar with implications for subduction zone magmas. Am Mineral 63: 641–663

Stern CR, Futa K, Muehlenbachs K (1984) Isotope and trace element data for orogenic andesites from the Austral Andes. In: Harmon RS, Barreiro BA (eds) Andean magmatism: chemical and isotopic constraints. Shiva Publishing, Cheshire, pp 31–46

Stern CR, Saul S, Skewes MA, Futa K (l989) Garnet peridotite xenoliths from the Pali-Aike basalts of southernmost South America. Spec Publ Geol Soc Aust 14: (2) 735–744

Stern CR, Frey FA, Futa K, Zartman RE, Peng Z, Kyser TK (1990) Trace element and Sr, Nd, Pb, and O isotopic composition of Pliocene and Quaternary alkali basalts of the Patagonian plateau lavas of southernmost South America. Contrib Mineral Petrol 104: 294–308

Sun SS, McDonough WF (1989) Chemical and isotopic systematics of oceanic basalts: implications for mantle composition and processes. In: Saunders AD, Norry MJ (eds) Magmatism in Ocean Basins. Geol Soc London Spec Pub 42: 313–345

Wolf MB, Wyllie PJ (1994) Dehydration melting of amphibolite at 10 kbar: the effect of temperature and time. Contrib Mineral Petrol 115: 369–383

Wyllie PJ, Wolf MB (1993) Dehydration melting of solid amphibolite at 10 kbar: textural development, liquid interconnectivity and applications to segregation of magmas. Mineral Petrol 44: 151–179

Yogodzinski GM, Kay RW, Volynets ON, Loloskov AV, Kay SM (1995) Magnesian andesite in the western Aleutian Komandorsky region: implications for slab melting and processes in the mantle wedge. Geol Soc Am Bull 107: 505–519